A DISSERTATION FOR
THE DEGREE OF DOCTOR OF PHILOSOPHY

Identification of *SPLIT-HULL* (*SPH*) and *LARGE EMBRYO* (*LE*) Genes in Rice (*Oryza sativa* L.)

BY

GILEUNG LEE

FEBURARY, 2018

MAJOR IN CROP SCIENCE AND BIOTECHNOLOGY
DEPARTMENT OF PLANT SCIENCE
THE GRADUATE SCHOOL OF SEOUL NATIONAL UNIVERSITY

Identification of *SPLIT-HULL* (*SPH*) and *LARGE EMBRYO* (*LE*) Genes in Rice (*Oryza sativa* L.)

UNDER THE DIRECTION OF DR. HEE-JONG KOH
SUBMITTED TO THE FACULTY OF THE GRADUATE SCHOOL
OF SEOUL NATIONAL UNIVERSITY

BY
GILEUNG LEE

MAJOR IN CROP SCIENCE AND BIOTECHNOLOGY
DEPARTMENT OF PLANT SCIENCE
NOVEMBER, 2017

APPROVED AS QUALIFIED DISSERTATION OF GILEUNG LEE
FOR THE DEGREE OF DOCTOR OF PHILOSOPHY
BY THE COMMITTEE MEMBERS
JANUARY, 2018

CHAIRMAN _____
Byon-Woo Lee, Ph.D.

VICE-CHAIRMAN _____
Hee-Jong Koh, Ph.D.

MEMBER _____
Hak Soo Seo, Ph.D.

MEMBER _____
Do-Soon Kim, Ph.D.

MEMBER _____
Joong Hyoun Chin, Ph.D

Identification of *SPLIT-HULL* (*SPH*) and *LARGE EMBRYO* (*LE*) Genes in Rice (*Oryza sativa* L.)

GILEUNG LEE

GENERAL ABSTRACT

Rice (*Oryza sativa* L.) is one of the most important cereal crop in the world. It is a primary food source of more than 90% of Asia and half of the world's population. Since the edible part of rice is the grain (kernel), development of a grain from floral organs formation to grain filling is one of the most important topics in rice research and breeding. In this study, we characterized *split-hull* (*sph*) and *large embryo* (*le*) mutant and conducted map-based cloning to identify genes related to grain development and possibility on utilization of these genes to rice breeding.

Rice grain is divided into two parts, the hull and the kernel. Rice hull consisting of two bract-like structures, the lemma and the palea, protects the seeds from environment and determines kernel shape and size. The *sph* mutant showed hull splitting in interlocking part of lemma and palea during grain filling stage.

Morphological and chemical analysis revealed that reduction in the width of the lemma and lignin content of the hull in the *sph* mutant might be the cause of hull-splitting. *SPH* was located in chromosome 4 and encoded type-2 13-lipoxygenase. *SPH* was expressed in leaf, stem, root, and spikelet, and interestingly, intensive expression was detected in the inner part of marginal region of lemma. The knock-out and knock-down transgenic plants showed split hull phenotype, and *sph* mutant contained significantly higher linoleic and linolenic acids (substrates of lipoxygenase) in spikelets than those of wild type. These results suggest that lipoxygenase (SPH) is involved in hull development and maintenance, and the genetic defect of lipoxygenase causes hull splitting phenotype. In dehulling efficiency test, the *sph* mutant showed high dehulling efficiency even by a weak tearing force in a dehulling machine, which suggests that hull splitting character might facilitate improving dehulling efficiency of fragile rice and breeding of easy-dehulling rice.

Rice embryo occupies a very small part of grain, but it contains various functional nutrients. Regulation of embryo size is an attractive breeding strategy to obtain dramatic improvement of rice nutritional quality. In the second chapter, three giant embryo mutants which were named according to the degree of embryo size enlargement as *le*, *ge*, and ge^{s}, from mild to severe, were morphologically and genetically characterized. They showed variation in embryo size, which was positively correlated with γ-aminobutyric acid (GABA) content. Allelism test and

sequence analysis of *GIANT EMBRYO* (*GE*) locus revealed that *ge* and ge^{s} were allelic to *GE* which was previously reported as the gene controlling embryo size, whereas the enlarged embryo phenotype of *large embryo* (*le*) is controlled by a novel gene. Through map-based cloning, *LE* locus was delimited to the 51.8 kb region in chromosome 3, and one nucleotide deletion was detected in the 12^{th} exon of *OS03g0706900* encoding C3HC4-type RING finger protein. To investigate the suppression effect of *LE* gene, knock-down transgenic plants were generated and showed enlarged embryo seeds, suggesting that C3HC4-type RING finger protein is participated in the regulation of embryo morphology. *LE* was expressed in all organs examined such as leaf, stem, root, and predominantly in 20 DAP seed. Our findings provide the basis of new regulation mechanism determining embryo size and will facilitate the development of new giant embryo cultivars for improving nutritional quality of rice.

Keyword: Rice, Grain, Map-based cloning, Split hull, Giant embryo, Large embryo.

Student Number: 2013-30325

CONTENTS

CHAPTER Π.

Identification of the *LARGE EMBYRO* (*LE*) Gene Controlling Embryo Size in Rice

LIST OF TABLES

LIST OF FIGURES

LIST OF ABBREVIATIONS

SPH	Split-hull
HSC	Hwaseonchal
LOX	Lipoxygenase
PUFA	Poly unsaturated fatty acid
LA	Linoleic acid
LeA	Linolenic acid
MNU	*N*-methyl-*N*-nitrosourea
DAF	Days after flowering
BSA	Bulked segregant analysis
SNP	Single nucleotide polymorphism
InDel	Insertion/deletion
ORF	Open reading frame
RACE	Rapid amplification of cDNA ends
RNAi	dsRNA-mediated interference
cTP	Chloroplast transit peptide
qRT-PCR	Quantitative real time PCR
mrl	Marginal region of lemma
mrp	Marginal region of palea
HC	Hwacheong
GE	Giant embryo
GO	Goliath
LE	Large embryo
GABA	γ-aminobutyric acid

CAPS	Cleaved amplified polymorphic sequences
dCAPS	Derived cleaved amplified polymorphic sequences
DAP	Days after pollination

LITERATURE REVIEW

Development of floral organs in rice

Rice, a type of grass, has unique structure of the floral architecture that has greatly diverged from those of eudicots. Rice spikelet which is the floral unit has a fertile floret, hull (lemma and palea), and a pair of sterile lemmas (also known as ‘empty glumes’), together with a pair of rudimentary glumes. Rice has perfect flower (floret) which is composed of six stamens and a carpel. It also contains two lodicules at the base of the pistil (Smith and Dilday 2003). In the place of sepals of eudicots, rice has evolved the lemma and palea, two brack-like structures that enclose the inner reproductive organs (Lombardo and Yoshida 2015). Floral organ development mechanism has been well studied and established as ABC model (further extended to the ABCDE model) in eudicots (Krizek and Fletcher 2005; Aceto and Gaudio 2011), which is applicable to rice spikelet development. In addition, distinctive mechanism also regulates floral organs of grass, especially outer organs such as lemma and palea (Yoshida and Nagato 2011; Lombardo and Yoshida 2015).

Free-dehulling (threshing) character in cereal crop

In cereal crop, easy dehulling process is a primary agronomic trait because it is directly linked to its edibility and loss of caryopses. In barley, a grain type is

classified into two categories, namely, hulled and naked grain. Hulled barley has hulled caryopses character in which the hull is firmly adherent to the grain as it matures, while naked barley has caryopses with easily separable hull. The naked caryopsis is controlled by a single gene, (*nud*, for nudum) located on the long arm of the 7H chromosome (Fedak et al. 1972). *Nud* encodes ethylene response factor (ERF) family transcription factor which has homology to the Arabidopsis *WIN1*/*SHN1* transcription factor gene controlling lipid biosynthesis pathway. This gene acts in the formation of epidermal lipid layer on the caryopsis, resulting in the adhesion between hull and caryopsis (Taketa et al. 2008). In wheat, the meaning of the term “hulled” is somewhat different compared with barley, because hull-caryopsis adhesion is not observed in wheat, but wheat is also classified in to hulled wheat and naked wheat. The naked grain trait is linked to the *Q* gene which shows high similarity to the members of the *APETALA2* (*AP2*) transcription factor family (Faris and Gill 2002; Faris et al. 2003). Recent molecular analysis of several di- and polyploid wheat species revealed that *Q* gene variations such as coding mutation (329Val/Ile), promoter variability, and substitution at microRNA172 binding site contribute to the formation of free-threshing phenotype in naked wheat (Simons et al. 2006; Sormacheva et al. 2014; Debernardi et al. 2017). In oat, distribution and amount of lignin is more restricted in naked oat than in hulled oat, which causes a formation of thinner and less rigid lemma in naked oat (Ougham et al. 1996). Genetic studies with the naked trait revealed that this trait is controlled by one major

gene termed *Naked1* (*N1*) with the action of three or four modifying genes depending on the analyzed genetic background (Ubert et al. 2017). However, a study on the easy-dehulling (threshing) trait has not been reported in rice.

Lipoxygenase

Lipoxygenases (LOXs) are nonheme iron containing fatty acid dioxygenases encoded by a large gene family found in all plants and animals. LOXs catalyze the deoxygenation of poly unsaturated fatty acids (PUFAs) containing a (Z,Z)-1,4-pentadien system (Siedow 1991). The catalytic cascade processes of PUFAs which consist of initial oxygenation catalyzed by LOXs and subsequent catalytic reactions, are collectively referred to as the LOX pathway. The LOX pathway comprising seven distinct branches generates a multitude of oxylipins, such as divinyl ethers, leaf aldehydes, leaf alcohols, ketols, and jasmonic acid. The oxylipins function as potent bio-regulators involved in plant growth and development, signaling cascades, senescence, organogenesis, and the maintenance of homeostasis (Grechkin 1998). Since all catalytic cascade processes in branches of the LOX pathway are preceded by LOXs catalysis, LOXs are very essential to regulate environmental responses and developmental processes in plants (Feussner and Wasternack 2002). The roles of LOXs have been investigated in rice, such as responses to wounding and insect attack, seed longevity and storage, and the production of stale flavors (Ohta et al. 1991; Suzuki et al. 1999a; Zhou et al. 2014; Huang et al. 2014).

Jasmonate

Jasmonates (JAs), lipid-derived hormone, play essential roles in plant, such as development and growth including senescence, germination, trichome initiation, tuber and floral organ formation, and defense response (Wasternack and Hause 2013). JA biosynthesis is carried out through the allene oxide synthase (AOS) branch included in lipoxygenase (LOX) pathway. The biosynthesis of JA is initiated in chloroplast, involving the release of poly unsaturated fatty acids (PUFAs), and subsequent oxygenation of PUFAs by LOXs. In the AOS branch of LOX pathway, only linolenic acid (LeA) is utilized as substrate in catalytic cascade. The LeA is transformed to 13-hydroperoxy octadecatrienoic acid (13-HPOT) by LOX-catalyzed peroxidation. This intermediate compound is dehydrated by AOS, and subsequently cyclized to racemic 12-oxo-phytodienoic acid (OPDA) by allene oxide cyclase (AOC). Subsequently, the OPDA is transferred to peroxisomes, where it is transformed to (+)-7-iso-JA by OPDA reductase (OPR) and three further β-oxidation steps (Yan et al. 2013). Several studies demonstrated that floral organ development is affected by JA biosynthesis and JA signaling. In Arabidopsis, the mutant of *DEFECTIVE IN ANTHER DEHISCENCE1* (*DAD1*) gene, liberating of PUFA from chloroplast membrane, showed defects in anther dehiscence, pollen maturation, and flower opening. These defects were rescued by exogenous application of JA or LeA (Ishiguro et al. 2001). Likewise, several studies using loss of function mutants of JA biosynthesis related genes such as *AOS* and *OPR* displayed defect of fertility and

reproductive organ development, and were rescued by JA application (Park et al. 2002; von Malek et al. 2002; Stintzi and Browse 2000). Overexpression lines of *TIFY* showed increased floret number and reduced spikelet fertility, and the loss of function mutants of *OsJAZ1* showed altered floral organ identities and numbers. (Cai et al. 2014; Hakata et al. 2017). In RNA expression analysis, exogenous application of methyl JA (MeJA) coordinately induced genes related to lignin biosynthesis in oat and Arabidopsis (Salzman et al. 2005b; Pauwels et al. 2008).

Rice grain anatomy

Rice grain consists of a hull and caryopsis. The dehulled rice grain is called ‘brown rice’ which contains the embryo and endosperm, covered by the pericarp, seed coat (tegmen), and aleurone layers, which collectively referred to as ‘bran’. The hull (husk) constitutes about 20 % of the rice grain and consists of hard materials such as silica and lignin. It protects the inner reproductive organs and caryopsis during rice growing season and is removed during the milling process. Although rice hull is considered as waste product in agriculture sector, it can be used as valuable raw materials in various industries (Kumar et al. 2013). The endosperm constitutes the largest portion of the rice caryopsis and is comprised of starch storage tissue, filled with starch granules and a small number of protein bodies (Champagne et al. 2004). The embryo is the rudimentary plant tissue that will grow up to be rice plant. Embryo is about 1-3 % by weight of total grain and consists of scutellum, embryonic

axis (plumule [leaf], hypocotyl [stem], and radicle [root]), and various structures that sheath the embryo (Champagne et al. 2004).

Rice embryo mutants

To date, a series of mutants affecting the embryo development and size have been reported (Satoh and Omura 1981a; Kim et al. 1991; Hong et al. 1995a). Hong et al. (1995a) identified 188 embryo mutants and categorized embryo mutants into six groups including embryoless, deletion of organ(s), abnormal position of organs, modified embryo size, morphological aberration, and variable abnormalities. The *embryoless* mutants had well-developed endosperm with a very small globular embryo. One of the mutants, the *embryoless 1* (*eml1*) showed temperature-dependently phenotype change (Hong et al. 1995b). The *globular embryo* (*gle*) mutants performed globular shape embryo without any developed embryonic organs. In *club-shaped embryo* (*cle*) mutants, vascular bundles were differentiated without formation of shoot and radicle. The *shootless* (*shl*) and *radicless* (*ral*) mutants failed to develop shoot and radicle in embryo, respectively. The *shoot organization1* (*sho1*) mutants showed defect in development of the first to third leaves with normal radicle. In embryo size mutant, two types of mutants developing either a reduced or enlarged embryo were reported (Hong et al. 1996). The *giant embryo* (*ge*) mutants had enlarged scutellum with normal size of shoot and radicle. The *reduced embryo* (*re*) mutants exhibit a reduction in the embryo size including reduction in all

embryonic organs and enlarged endosperm (Hong et al. 1996). Double mutants analysis of *ge* and *re* revealed that *RE* acts upstream of *GE* in embryo-facing endosperm (Nagasawa et al. 2013).

Giant embryo rice

Rice embryo accounts for only 2-3% of total seed weight. However, it contains various nutrients and bioactive sources, such as protein, fat, vitamins, γ-aminobutyric acid (GABA), α-tocopherol, and γ-oryzanol. To improve nutritional quality of rice, giant embryo mutants have been used as breeding materials. (Maeda et al. 2001; Takahashi et al. 2009; Hong et al. 2012a; Han et al. 2012a; Chung et al. 2013; Sakata et al. 2016). Brown rice of giant embryo rice contains significantly higher crude lipid, crude protein, vitamins (B1, B2, and E), some essential amino acids, fatty acids, mineral elements (Ca, Fe, Mg, K, P, and Zn), and γ-oryzanol than those of normal rice (Zhang et al. 2005; Jeng et al. 2012; Kim et al. 2013). In addition, GABA content in giant embryo rice is higher than in normal rice, and is more accumulated during water-soaking and germination (Liu et al. 2005; Choi et al. 2006; Zhao et al. 2017). In dietary experiments, brown rice of giant embryo rice exhibits greater body fat-lowering effects and antioxidant potential than those of normal rice (Chung et al. 2013; Chung et al. 2014a; Chung et al. 2016b; Chung et al. 2016a).

CHAPTER I

Identification of a Novel Gene *SPLIT-HULL* (*SPH*) Associated with Hull Splitting in Rice

ABSTRACT

Rice hull consists of two bract-like structures, the lemma and palea. The hull is an important organ that helps to protect seeds from environmental stress, determines seed shape, and ensures grain filling. Achieving optimal hull size and morphology is beneficial for seed development. Therefore, understanding rice hull development is important for obtaining high-quality grains with normal grain filling. The rice *split-hull* (*sph*) mutant exhibits hull splitting in the interlocking part of the lemma and palea and/or the folded part of the lemma during the grain filling stage. Morphological and chemical analysis revealed that the reduction in the width of the lemma and lignin content of the hull in the *sph* mutant might be the cause of hull-splitting. Genetic analysis indicated that the mutant phenotype was controlled by a single recessive gene, *sph* (*Os04g0447100*), which encodes a type-2 13-lipoxygenase. *SPH* knockout and knockdown transgenic plants displayed the split hull phenotype, as shown in the *sph* mutant. The *sph* mutant contained significantly higher linoleic and linolenic acids (substrates of lipoxygenase) in spikelets than

those of wild type. It might be due to a genetic defect of *SPH* and subsequent decrease in lipoxygenase activity. In dehulling experiment, the *sph* mutant showed high dehulling efficiency even by a weak tearing force in a dehulling machine. Our findings provide a basis for better genetic understanding of the role of lipoxygenase activity in hull structure and maintenance and would facilitate breeding the easy-dehulling rice cultivar.

Keyword: Rice, *SPH*, Split hull, Hull size, Lipoxygenase, Lignin

INTRODUCTION

Rice (*Oryza sativa* L.) is one of the most important cereal crops worldwide. Since the grains of this crop are mainly utilized, the development of floral organs such as hull and reproductive organs should be considered as a crucial factor that directly affects grain development. Rice hull protects seeds from the external environment during the growing season and maintains the proper humidity levels inside the spikelet. The size and shape of the hull, which limit seed growth, are important factors that help to determine grain size and filling rate, thereby affecting grain yield and quality (Fu et al. 2015).

The basic model of floral organs formation, the so-called ABC or ABCDE model, has been well studied in eudicots, such as *Arabidopsis thaliana* and *Antirrhinum majus*. An Arabidopsis flower has four concentric whorls of floral organs in the following order: sepals, petals, stamens, and carpels. The development of each part is controlled by groups of genes, such as class A, B, C, D, and E genes (Schwarz-Sommer et al. 1990; Krizek and Fletcher 2005). Unlike eudicots, the floret or spikelet is the structural unit of a flower in grass, which contains stamens, carpel, and distinctive organs such as lodicules and bract-like structures consisting of lemma and palea. The mechanism of floret development in grasses is similar to the basic model of flower development in eudicots, but this process is also regulated by

specific genetic mechanisms due to the distinctive organs in these flowers (Yoshida and Nagato 2011). Whether the lemma and palea are part of the perianth or non-floral organs is currently under debate. The disruption of *SILKY1*, a class B gene, leads to the conversion of lodicules (petal equivalents) into lemma/palea-like structures in maize (Ambrose et al. 2000). In a loss of function rice mutant of *SUPERWOMAN1* (*SPW1*)/*OsMADS16*, a homolog of an Arabidopsis class B gene, floral organs are transformed from stamens and lodicules into carpels and palea-like organs (Nagasawa 2003). These studies suggest that lemma and palea are equivalent to sepals.

Many studies have been conducted to examine the regulatory mechanisms and to isolate the genes related to hull development in rice (Chen et al. 2006; Wang et al. 2010b; Yoshida and Nagato 2011; Huang et al. 2013; Wang et al. 2015; Si et al. 2016; Yu et al. 2017). Lemma and palea can be distinguished by their diverse morphological features, such as the number of vascular bundles and the morphology of the marginal region structure. The identities of lemma and palea are determined by each of the organ-specific mechanism, together with common development mechanism. *RETARDED PALEA1* (*REP1*) regulates palea identity and development in rice. The palea of the *rep1* mutant exhibits retarded development and contains five vascular bundles, like the lemma (Yuan et al. 2009). Likewise, the *mosaic floral organs1* (*mfo1*) mutant displays slightly enlarged palea and an inwardly curled marginal region of palea (mrp) (Ohmori et al. 2009). On the other hand, *LEMMA*-

DISTORTION1 (*LD1*) specifically affects the morphology of the lemma. In the *lemma-distortion1* (*ld1*) mutant, the lemma shows distorted phenotypes, whereas the palea exhibits normal morphology (Yang et al. 2016).

Lee et al. (2004) described a *split-hull* (*sph*) mutant in rice that is controlled by a single recessive gene. In this study, we further characterized this mutant and isolated the responsible gene to reveal the reason of hull splitting and identify the possibility of utilization of this mutant on rice breeding.

MATERIALS AND METHODS

Plant materials

The *sph* mutant was induced from *japonica* cultivar Hwaseonchal (HSC) mutagenized with *N*-methyl-*N*-nitrosourea (MNU) (Lee et al. 2004). HSC was used as the wild type in comparing phenotypic data. Milyang 23, a Korean *Tongil*-type cultivar, was crossed with *sph* mutant to construct the mapping population. Dongjin, a *japonica* cultivar, was used to generate transgenic plants and used as the control of transgenic lines. To validate the gene function of *sph*, T-DNA tagging line (PFG_3A-05276) was shared by Prof. Gynheung An (Kyung Hee University, Korea). All plant materials were grown at the Experimental Farm Seoul National University (Suwon, Korea) under normal cultivation conditions.

Phenotypic analysis

The dimensions of the hull and dehulled seeds were measured from microscopic images with HD'MEASURE software (HANA Vision, Korea). To obtain accurate measurements of lemma and palea size, separated lemma and palea were mounted onto a glass slide and covered, then pressed with another glass slide. Hull weight and TGW were measured with an electronic balance (CAS, USA). Plant morphological traits were measured at heading stage and grains and panicle related traits were measured after harvest when grains were fully ripened.

Genetic analysis and fine mapping of *SPH*

For genetic segregation analysis, the F_2 population derived from a cross between *sph* mutant and HSC was grown in the paddy field and its segregation ratio was analyzed. Other F_2 and F_3 populations derived from a cross between *sph* mutant and Milyang 23 were used for gene mapping. For BSA, F_2 plants showing the split hull phenotype were selected and used to make mutant bulk DNA. BSA was performed using the Fluidigm SNP genotyping platform (Fluidigm Cor., USA), using 159 polymorphic SNP markers evenly distributed in the rice genome. Fine mapping was performed using newly designed InDel and SNP markers. Newly designed primers for mapping are listed in Table 1.

Statistical analysis

Statistical analysis of phenotypic data and expression data was conducted using IBM SPSS Statistics software version 24 (IBM, USA). The segregation ratio of F_2 population derived from a cross between *sph* mutant and HSC was statistically analyzed for deviation from the expected Mendelian segregation ration (3:1) by x^2 test using Excel 2013 (Microsoft Corp., USA).

Cell wall composition analysis

Hulls from HSC and *sph* mutant were ground to a fine powder and dried. To determine the content of cellulose and lignin, acid detergent fiber (ADF) form the

samples was investigated using ANKOM2000 (ANKOM Technology Corp., USA). The samples sealed with filter bag were agitated and heated in acid detergent solution (20g of cetyl trimethylammonium brobide (CTAB) added into 1N H_2SO_4) for 1 hour. After exhausting hot solution, samples were rinsed using hot H_2O for 5 mins. Repeat rinses for a total of three times and soak in acetone for 3 mins. After dry of samples, the % of remained sample weight (ADF) was calculated exactly. After performing ADF determinations, the ADF was soaked in 72% H_2SO_4 for 3 hours and rinsed with tap water and acetone to remove all acids, followed by drying and weighing. After ashing the samples, the acid detergent lignin (ADL) was weighed. Cellulose and lignin contents were determined using the following formula: cellulose (%) $= (W2 - W3)/W1$, lignin (%) $= W4/W1$ W1 = sample weight, W2 = ADF, W3 = ADF (treated H_2SO_4), W4 = ADL. Total silica (SiO_2) contents in hull samples were determined gravimetrically using hydrofluoric acid evaporation (Kolthoff and Sandell 1952).

Candidate gene analysis

To identify the nucleotide changes and splicing pattern in the candidate gene, DNA fragments of the gene were amplified by PCR from gDNA and cDNA. PCR products were purified using a PCR Purification kit (Inclone, Korea) and ligated to pGEM-T Easy Vector (Promega, USA), followed by transformation into *E. coli* strain DH5α. Transformed plasmid sequences which were purified by Plasmid

Purification kit (Inclone, Korea) were analyzed with an ABI Prism 3730 XL DNA Analyzer (PE Applied Biosystems, USA) and aligned using CodonCode Aligner software (CodonCode Corporation, USA). The information of the primers for amplification of DNA fragments is listed in Table 1.

Multiple sequence alignment and phylogenetic analysis

The amino acid sequences of LOX protein were downloaded from the Universal Protein Resource (UniProt, http://www.uniprot.org). Multiple sequence alignment was carried out using Probcons, and background color shading was applied with Jalview using the % identity scheme. Arabidopsis, maize, soybean, potato, and rice LOX amino acid sequences (Table 1-2) were aligned with Probcons, and a neighbor-joining tree was constructed with MEGA 6 software via the bootstrap method with 1000 replicates. The presence of a cTP was predicted with ChloroP (Emanuelsson et al. 1999).

Histological analysis

Spikelets of HSC and *sph* mutant at the heading stage were fixed in formalin-acetic acid-alcohol (FAA) fixative buffer (3.7% formaldehyde, 5% acetic acid, 50% ethanol) at 4°C overnight, followed by dehydration and subsequent infiltration with Paraplast® (Sigma, USA). The paraffin-infiltrated samples were embedded in an embed block and cut into 5 μm sections with an HM 340 E Rotary Microtome

(Microm Lab, Germany). The sections were stained with 0.25% toluidine blue O (Sigma, USA) and examined by optical microscopy.

Fatty acid analysis

LA and LeA contents were estimated using the one step-lipid extraction and methyl ester method (Garces and Mancha 1993), with slight modifications. FAMEs were prepared from ground spikelet samples treated with a methylation mixture (Methanol : Benzene : DMP : H_2SO_4 = 39 : 20 : 5 : 2) and heptane. Quantification of FAMEs was carried out by gas chromatography on an Agilent 7890A (Agilent, USA) with a DB-23 column, 60m × 0.25 mm × 0.25 μm (Agilent, USA). Fatty acid levels were calculated using an internal standard (pentadecanoic acid, C15:0).

RNA extraction, RACE, and qRT-PCR analysis

Total RNA was extracted from leaf, stem, root, and spikelet tissue using RNAiso plus (Takara Bio, Japan), and the extracted RNAs were treated with RNase-free Recombinant DNase I (Takara Bio, Japan) to eliminate genomic DNA contamination. First-strand cDNA was synthesized using M-MLV reverse transcriptase (Promega, USA). qRT-PCR was performed using SYBR premix ExTaq (Takara, Japan) on a CFX96™ Real-Time PCR system (Bio-Rad, USA) according to the manufacturer's instructions. To identify the start codon and splicing pattern of *SPH*, 5'RACE was performed using a SMARTer® RACE 5'/3' kit

(Clontech, USA). The primers for qRT-PCR and 5'RACE are listed in Table 1-1.

GUS staining

GUS staining was carried out as previously described (Jefferson et al. 1987). The GUS staining solution was vacuum-infiltrated into various organ samples for 10 minutes. The samples were incubated overnight at 37°C in staining solution, followed by incubation in 90% ethanol overnight at room temperature to bleach the chlorophyll in the samples.

Vector construction and transformation

The promoter region and 3'UTR (including the CDS) of *SPH* was amplified by PCR, and each PCR product was cloned into pHGWFS7 and pH7GWIWG2(II), respectively, using Gateway® BP and LR Clonase™ II enzyme mixes (Invitrogen, USA). The final constructs were introduced into Dongjin, a *japonica* cultivar, through transformation with *Agrobacterium* strain LBA4404. Transformation was carried out using a previously published *Agrobacterium*-mediated transformation method (Nishimura et al. 2007) with slight modifications. The primers for cloning of target region are listed in Table 1-1.

Table 1-1. Information of the primers used in this study

Primer name	Purpose	Forward primer (5'→'3')	Reverse primer (5'→3')	Note
S04060	Mapping	TATGGTTTTATCCGCCAACC	GCTACAACTAAAACAAGAAACGTGA	InDel
S04070	Mapping	AAATGCTGACAAGTGAAGTGCT	AGCCATCGAGTGCTTGAAAT	InDel
M3	Mapping	TCAAATGAAGCTGTACAAGAAG	TAGTACAACGGAGTTTAAGCAA	InDel
M6	Mapping	GGAGTAGCATTTTCTGGGTGAC	GGCACCATATGCTCTCATGTTA	InDel
M9	Mapping	CGCATGTCAGTGGCTGATACTA	CTCACGAACCTGAGACTCCTCT	InDel
M10	Mapping	GGAGACCGACCCAAGTAAGC	GAGGGGCATGGAATTCTAAA	InDel
C1	Mapping	TTCGGGGAAACTTGCATATC	GGATGAACATCCATCCGTTT	CAPS
C2	Mapping	TCACTCTCCATTGGGTAGGTCTA	CTTGCCACAGGTTAGATAAGCA	CAPS
M12	Mapping	GGCCGTCTTCAGAAAGACTTGT	GGGTAATTTGAAGCTGAAATGG	InDel
SPH-1	*SPH* gene sequencing	TCTCGGGCAAAGGAGTGTTGGA	GCCTTGACGTCCTTCTTGTC	-
SPH-2	*SPH* gene sequencing	CGATCGGAATTGATCATGTG	CTCCGACAGCATCTCGTTCT	-
SPH-3	*SPH* gene sequencing	AGTACCCGGAGCCCATCTAC	GATGTCGTGGTAATCCAGCA	-
SPH-4	*SPH* gene sequencing	AGTGGAGCTGATTGGTGGTC	ACGTGTACCTTCGGATGAGG	-
SPH-5	*SPH* gene sequencing	CGGTACACGCTCAAGATCAA	GTCATGAACGTCGTGGTCTG	-
SPH-6	*SPH* gene sequencing	GAGCTGCAGTCGTGGTACG	GCAATCGACCTATCCGAAGA	-
GSP1	5'RACE		CGGGAGGAAGATGTCGTGGTAATCC	-
qOsACT	qRT-PCR	TTCCAGCAGATGTGGATTGC	GCTTAGCATTCTTGGGTCCG	-
qSPH	qRT-PCR	CTGGTTGAGGACGCACGC	CCAGCGCGTTGATCTTGAG	-
3A-05267A	T-DNA insertion check	AGTGGAGCTGATTGGTGGTC		-
3A-05267C	T-DNA insertion check		ACGTGTACCTTCGGATGAGG	-
NGUS1	T-DNA insertion check	AACGCTGATCAATTCCACAG		-
sphRNAi	*SPH* RNAi transgenic line	AAAAAGCAGGCTACACGCTGTCCACGCACT	AGAAAGCTGGGTGCAATCGACCTATCCGAAGA	-
sphGUS	*SPH* GUS transgenic line	AAAAAGCAGGCTAGTAACCTGCTTCAAGGCCC	AGAAAGCTGGGTAGAAATCCCCTACGCTACAG	-

Table 1-2. Plant LOX sequences information used in phylogenetic analysis

Organism	Nomenclature in this study	Sequence length	UniProtKB accession
Oryza sativa	OsLOX1	926	Q6H7Q6
	OsLOX2	918	Q8H016
	OsLOX3	863	Q76I22
	OsLOX4	866	Q7G794
	OsLOX5	877	Q53RB0
	OsLOX6	870	P29250
	OsLOX7/SPH	922	-
	OsLOX8	847	Q0DJB6
	OsLOX9	924	P38419
	OsLOX10	941	Q84YK8
	OsLOX11	868	Q0IS17
	OsLOX12	922	Q2QNN5
	OsLOX13	450	Q2QNM6
Zea mays	ZmTS1	918	B8XH55
	ZMTS1b	916	B8XH56
	ZmLOX1	864	Q8W0V2
	ZmLOX2	873	Q9LKL4
Arabidopsis thaliana	AtLOX1	859	Q06327
	AtLOX2	896	P38418
	AtLOX3	919	Q9LNR3
	AtLOX4	926	Q9FNX8
	AtLOX5	886	Q9LUW0
	AtLOX6	917	Q9CAG3
Solanum tuberosum	StLOX1	844	Q9SAP1
	StLOX2	876	Q41430
	StLOX3	862	Q43191
	StLOX4	899	O24370
	StLOX5	914	O24371
Glycine max	GmLOX1	839	P08170
	GmLOX2	865	P09439
	GmLOX3	857	P09186
	GmLOX4	853	P38417
	GmLOX6	859	Q43440
	GmLOX7	864	P24095

RESULTS

Characterization of the *sph* mutant

The split-hull phenotype was observed in the interlocking part between the lemma and palea and folded part of the lemma during the grain filling period in the *sph* mutant (Fig. 1-1a-c). The hull-splitting of interlocking part initiated around 15 days after flowering (DAF) and was more clearly observed with the occurrence of tearing at the bottom part of the lemma while the grains were maturing and drying. There was an increased occurrence of abnormal spikelets, including elongated sterile lemma, the conversion of palea into lemma-like structure, elongated lodicule, and multiple pistils in the *sph* mutant (Fig. 1-1d and Table 1-3). In addition, the *sph* mutant showed early heading (approximately four days earlier than the wild type), increased culm length (CL), reduced spikelet number per panicle (SPP) and seed setting rate (SSR), and increased 1000-grain weight (TGW) compared with the wild type (Table 1-3, Fig. 1-2). These split and tearing hull characteristics made the hull to be easily separated from caryopsis, which facilitated high dehulling rate with less stress applied to the rice caryopses. In dehulling experiment with low tearing force, wild type grains showed about 20% dehulling rate after single pass dehulling process, while *sph* mutant grains showed more than three times higher dehulling rate than wild type (Fig. 1-3).

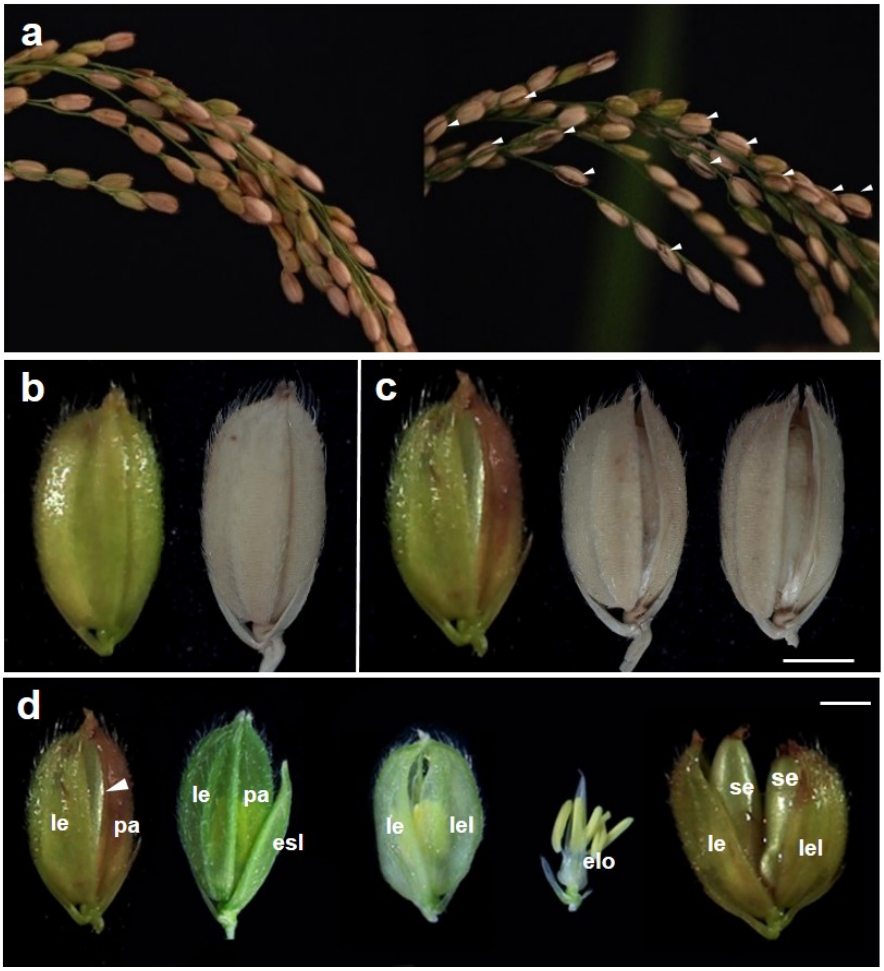

Figure 1-1. The panicle and grain phenotype of wild type and *sph* mutant. **a** Panicle of wild type (left) and *sph* (right) mutant. Grains of wild type (left, 15 DAF grain; right, mature grain) (**b**) and *sph* mutant (left to right: 15 DAF grain, mature grains) (**c**). **d** Abnormal spikelet and grain (20 DAF) morphology observed in *sph* mutant. le, lemma; pa, palea; esl, elongated sterile lemma; lel, lemma-like; elo, elongated lodicule; se, seed. White arrow heads indicate chasm generated by hull splitting. Scale bar = 2mm

Table 1-3. Phenotypic observation of agronomic traits between the wild type and *sph* mutant

	DTH	PH (cm)[NS]	CL (cm)[a]	PL (cm)[NS]	PN[NS]
wild type	105	100.4 ± 3.05	79.0 ± 3.26	20.6 ± 1.46	15.8 ± 3.31
sph	101	100.8 ± 3.48	83.9 ± 2.76	20.6 ± 1.28	15.6 ± 2.24
	SPP[b]	**SSR (%)[b]**	**TGW (g)[b]**	**ASR (%)[b]**	
wild type	105.3 ± 7.40	92.8 ± 3.22	21.7 ± 0.17	0.79 ± 0.72	
sph	94.6 ± 11.19	89.2 ± 3.54	23.0 ± 0.83	5.57 ± 2.34	

Data are given as means ± s.d ($n \geq 5$). Student's *t*-test was used to generate the *p* values. [a], $p < 0.05$. [b], $p < 0.01$. NS, not significant. DTH, days to heading; PH, plant height; CL, culm length; PL, panicle length; PN, panicle number; SPP, spikelet number per panicle; SSR, seed setting rate; TGW, 1000-grain weight (dehulled seeds); ASR, abnormal spikelet rate.

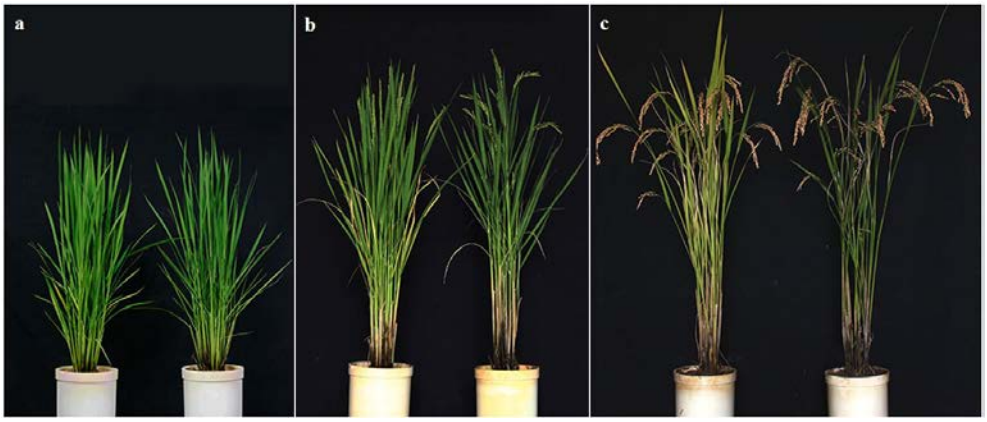

Figure 1-2. Plant morphology in wild type and *sph* mutant. Comparison of gross plant morphology between wild type (left) and *sph* mutant (right) at the vegetative (**a**), heading (**b**), and yellow ripe stages (**c**).

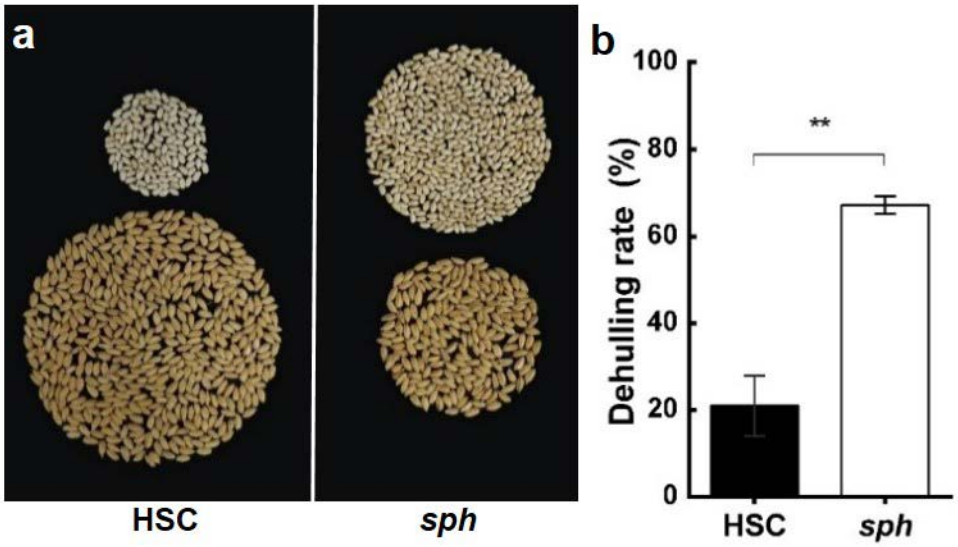

Figure 1-3. Comparison of dehulling efficiency between wild type and *sph* mutant. **a** Ratio of dehulled seed and paddy after single dehulling process with 2 mm distance between robber roller rice huller. **b** Comparison of dehulling rate between wild type (HSC) and *sph* mutant. Error bars indicate ±s.d. of replicates. Asterisks represent significant difference as determined two tailed student's *t*-test (*, $p < 0.05$; **, $p < 0.01$)

Morphological and physical property of hull and dehulled seed

The hull of *sph* mutant has fragile and weak hull causing hull splitting and tearing (Fig. 1-1a-c), and the hull weight of the mutant was significantly lighter than that of wild type (Fig. 1-4a). To confirm the physical properties of the hull, cell wall composition of hll was analyzed. There was no significant difference in cellulose or silica content between *sph* mutant and the wild type, but the lignin content was

significantly reduced in the mutant (Fig. 1-4b). To reveal the difference of morphological properties of grain between wild type and *sph* mutant, we measured the dimension of lemma, palea, and dehulled seed. Because the split hull phenotype was observed in approximately 47% of the *sph* mutant grains (Fig. 1-4c), *sph* mutant grains were classified into two categories according to grain type: *sph*-nor (normal-type dehulled seeds) and *sph*-sh (split hull-type dehulled seeds). In the comparison of hull size among a wild type and two *sph* types, the lemma widths of all *sph* types were significantly narrower than that of wild type. However, there was no significant difference between two *sph* types in every investigation of hull size (Fig. 1-4d). The *sph*-nor and *sph*-sh type showed significantly smaller width and larger thickness in dehulled seed than those of wild type, respectively (Fig. 1-4e-g). In histological analysis, we couldn't find any morphological defect in the interlocking part of the hull of *sph* mutant (Fig. 1-5). These results indicate that the hull splitting phenotype in the mutant was affected by hull size change and weak mechanical strength of the hull probably due to its low lignin content.

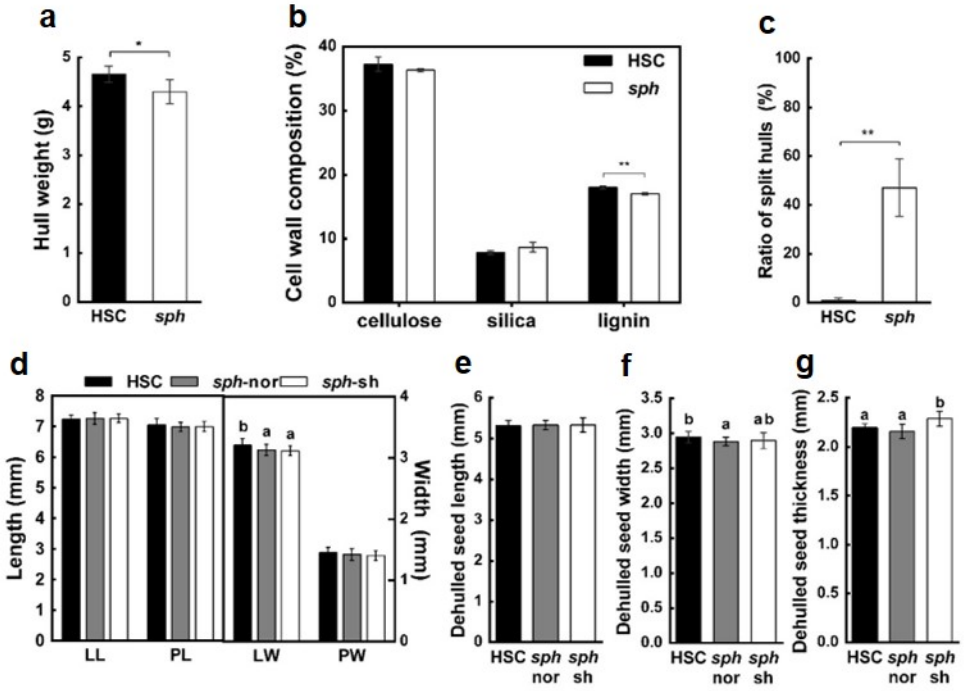

Figure 1-4. Comparison of hull and grain characteristics between wild type and *sph* mutant. **a** Hull weight of 1000 grains. **b** Cell wall composition of hull. **c** The percentage of split hull grain per panicle. **d** Length and width of lemma and palea. **e-g** The dimension of dehulled seed. *sph*-nor and *sph*-sh indicated dehullded seed from normal-type grain and split hull-type grain, respectively in *sph* mutant. LL, lemma length; PL, palea length; LW, lemma width; PW, palea width. Error bars indicate ±s.d. of replicates. Asterisks represent significant difference as determined two tailed student's *t*-test (*, $p < 0.05$; **, $p < 0.01$). Different lowercase letters mean significantly different ($p < 0.05$, one-way ANOVA) according to Tukey's post hoc test

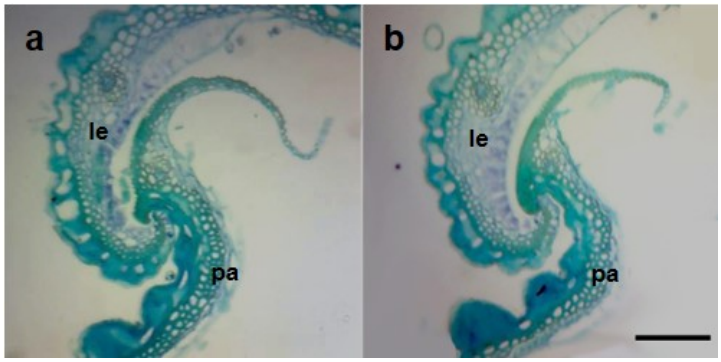

Figure 1-5. Histological analysis of interlocking part of spikelet. Magnified interlocking part between lemma (le) and palea (pa) in wild type (**a**) and *sph* mutant(**b**). Scale bar = 100um

Genetic analysis and map-based cloning of *SPH*

All the F_1 plants from a cross between *sph* mutant and HSC showed normal phenotypes. In F_2 population from the cross, F_2 plants were classified into two types of phenotype, one is normal type which didn't show hull splitting at all and the other is mutant type which showed hull splitting phenotype in ~47% of grains. The segregation ratio of normal and *sph* type plants was 3:1 (Table 1-4). It indicated that the *sph* mutant phenotype is controlled by a single recessive gene. Followed by Bulked segregant analysis (BSA), the *SPH* locus was found to be linked with a SNP marker (cmb0422.7) on chromosome 7. Next, fine mapping was conducted with newly designed InDel and CAPS markers using 383 F_2 and 251 F_3 plants. *SPH* was delimited within approximately 113-kb chromosomal region between M9 and C2

markers. We identified 27 predicted open reading frames (ORFs) in the candidate region (RAP-DB, version IRGSP 1.0; Fig. 1-6a). All ORFs of HSC and *sph* mutant were sequenced using their genomic DNA as templates, and the only one SNP in a LOX encoding gene, *Os04g0447100*, was identified. Due to the transcript form of *Os04g0447100* is incomplete, 5'rapid amplification of cDNA ends (5'RACE) and sequence analysis using cDNA were performed to identify the actual splicing pattern and transcription start site of this gene. The result of cDNA sequence analysis revealed that the transcript form of *SPH* was different from that of *Os04g0447100*. *SPH* was composed of seven exons and six introns and the start codon was determined with the first methionine (Met) residue fitting into the amino acid sequence frame (Fig. 1-6b, Fig. 1-7). The mutation occurred in the 2177th ORF nucleotide, where an adenine was substituted with a thymine, resulting in an amino acid change from aspartic acid (Asp) to valine (Val) in the *sph* mutant (Fig. 1-6c).

Table 1-4. Genetic segregation of the split hull trait in F_1 plants and F_2 population derived from the cross between the *sph* mutant and HSC

Cross combination	Generation	n	Ratio tested	No. of plants		Total	Chi-square (χ2)	*p*
				Normal	Split hull			
***sph* mutant /Hwaseonchal**	**F_1**	**8**	**-**	**8**	**0**	**8**	**-**	**-**
	F_2	**220**	**3:1**	**166**	**54**	**220**	**0.006**	**0.94**

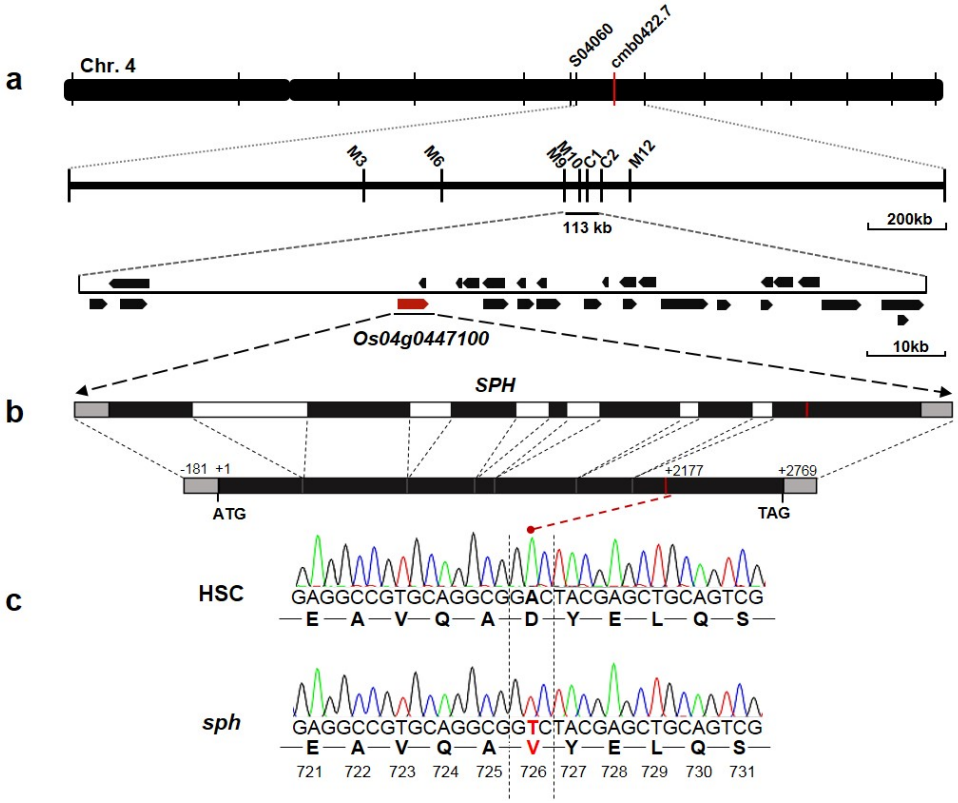

Figure 1-6. Map-based cloning of the *SPH* (*Os04g0447100*) gene. **a** Schematic diagram of the *SPH* gene cloning. **b** The *SPH* gene construction and splicing pattern. The gray, white, and black boxes indicate UTRs, introns, and exons, respectively. The mutation position is marked with a red line. **c** Sequence analysis of *SPH* gene.

Figure 1-7. Determined cDNA sequence of *SPH*. The arrow indicates the transcription start site (TSS), which was detected by 5'RACE and cDNA sequence analysis. The gene-specific primer used in 5'RACE is highlighted with a blue background. Start and stop codon are highlighted by open boxes. Black and red arrow-head indicate exon-exon junctions and the missense mutation in *sph*, respectively.

Validation of the mutation causing the split hull phenotype

To confirm that *SPH* is the gene associated with the split hull phenotype, dsRNA-mediated interference (RNAi) transgenic plants were developed, and the T-DNA tagging line (PFG_3A-05276) was employed. No expression of *SPH* was detected in knockout plants, in which T-DNA was inserted into the fifth intron of the gene (Fig. 1-8a). The T-DNA plants showed split hull grains (Fig. 1-8c), increased CL, and abnormal spikelet, which are the same characteristics observed in the *sph* mutant (Fig. 1-9a, d-i). RNAi plants with down-regulated *SPH* expression displayed the split hull phenotype (Fig. 1-8b, d). In addition, F_1 plants derived from reciprocal crosses between *sph* mutant and the T-DNA plant also displayed a split hull phenotype (Fig. 1-9b, c). These results demonstrate that the mutant phenotype is due to the loss of function of *SPH*.

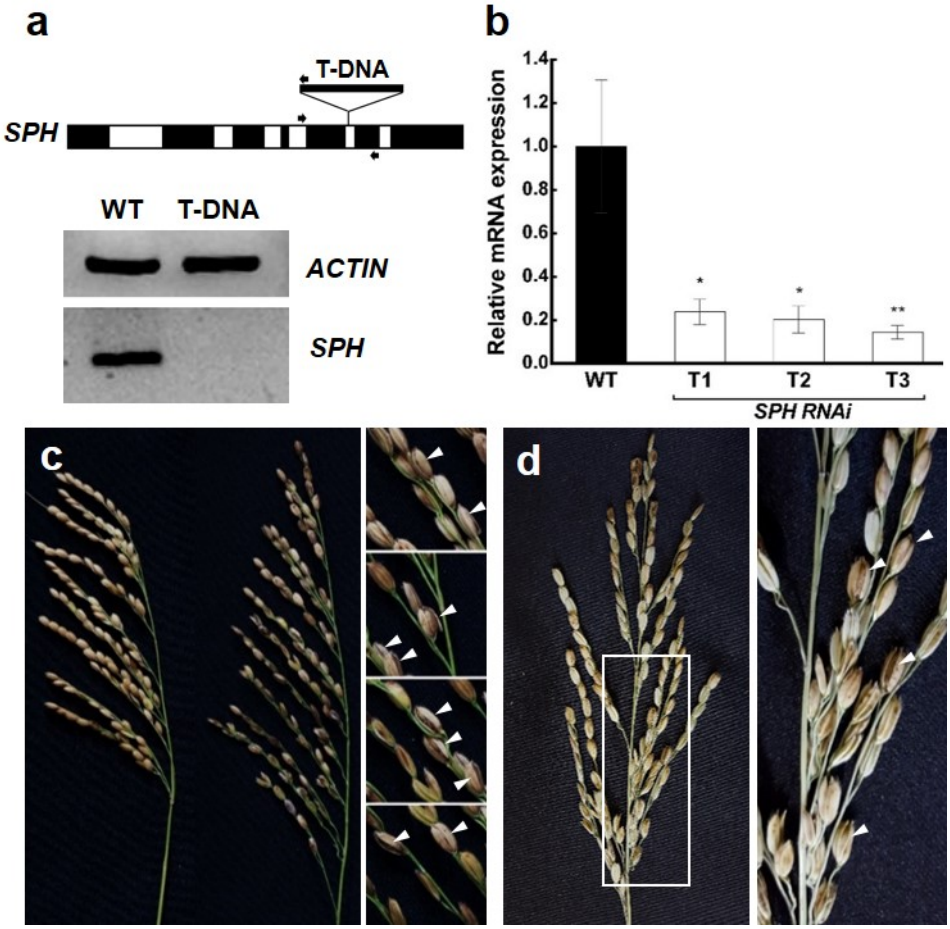

Figure 1-8. Phenotype and expression analysis of the RNAi and the T-DNA transgenic plants. **a** T-DNA insertion position in the *SPH* gene model and semi-quantitative RT-PCR analysis of *SPH* and *ACTIN* expression in the wild type (WT) and the T-DNA plant. **b** Relative expression of *SPH* (normalized to *ACTIN*) in WT and RNAi plants examined by qRT-PCR. Panicle and hull phenotypes of WT and T-DNA plant (**c**) and RNAi plant (**d**). Black arrows indicate primers used to examine T-DNA insertion. White arrow-heads indicate split hull grains. Error bars indicate ± s.d. of three replicates. Asterisks represent significant difference, as determined by a two-tailed Student's *t*-test (*, $p < 0.05$; **, $p < 0.01$).

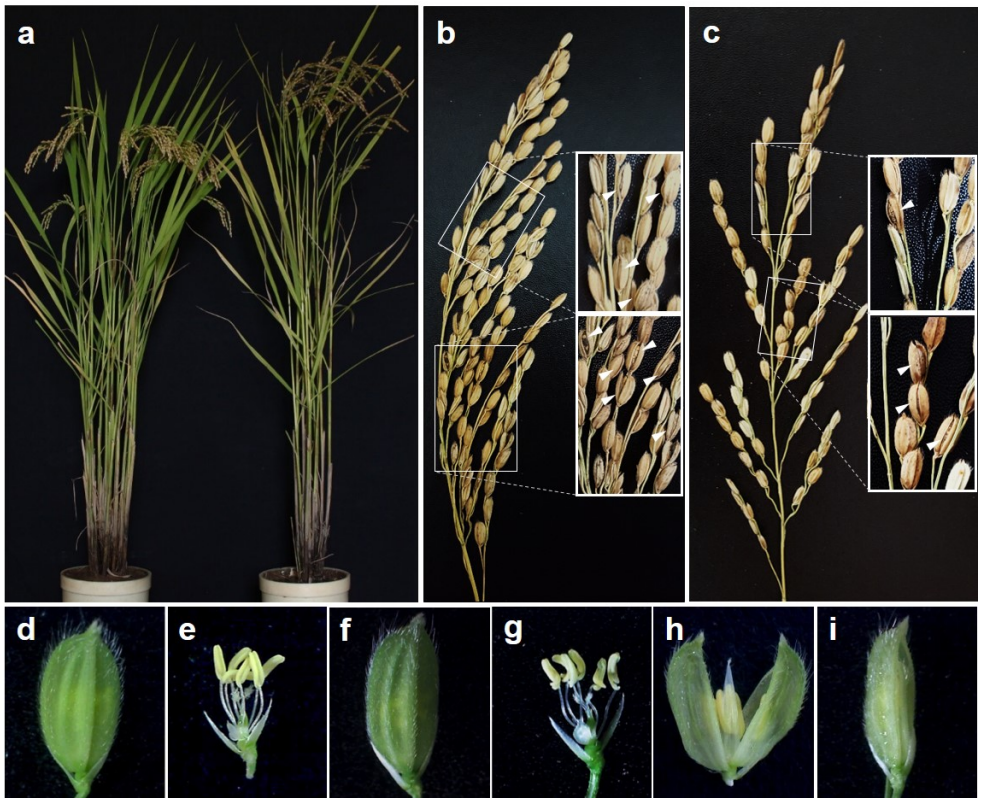

Figure 1-9. Phenotype of the T-DNA plant and allelism test by crossing the T-DNA plant with *sph* mutant. **a** Plant architecture of the T-DNA plant (left, wild type [Dongjin]; right, T-DNA plant). Panicle and spikelet phenotypes of F_1 plants derived from crosses of T-DNA plant × *sph* mutant (**b**) and *sph* mutant × T-DNA plant (**c**). Spikelet phenotypes of the wild type (**d**, **e**) and the T-DNA plant (**f-i**). White arrow-heads indicate split hull grains. Scale bar = 2 mm.

SPH encoding a type-2 13-LOX

The ORF of *SPH* is 2769 bp long (Fig. 1-7), encoding a deduced protein of 923 amino acids with a predicted molecular weight of 102.36 kDa. The SPH protein

contains two conserved domains: the PLAT/LH2 domain (plant lipoxygenase related protein domain) and the LOX superfamily domain. Multiple sequence alignment of LOX proteins showed that a significant portion of the amino acids in SPH are conserved among various plant species. LOXs can be classified into two groups, 9-LOX and 13-LOX, according to the positional specificity of oxygenation. SPH contains phenylalanine (Phe^{640}), the amino acid residue that determines the resiospecificity of 13-LOX (Liavonchanka and Feussner 2006). The 13-LOXs are subdivided into two types depending on the presence of a chloroplast transit peptide (cTP): type-1 13-LOXs lake a cTP, and type-2 contain a cTP. Using ChloroP (Emanuelsson et al. 1999), we found that SPH contains an N-terminal cTP (Fig. 1-10a), suggesting that SPH is a type-2 13-LOX. Phylogenetic analysis of plant LOXs showed that SPH is included in the type-2, 13-LOX group clade (Fig. 1-10b).

LOXs catalyze the dioxygenation of PUFAs such as linoleic acid (LA) and α-linolenic acid (LeA) (Feussner and Wasternack 2002). Since LA and LeA are substrates of LOX, we conducted quantitative analysis of these compounds to identify changes in enzyme activity in the *sph* mutant. Both the LA and LeA contents were conspicuously higher in *sph* mutant spikelets than those of wild type (Fig. 1-11a). These results indicate that the mutation in LOX domain reduces LOX enzyme activity, resulting in remaining substrates of LOX.

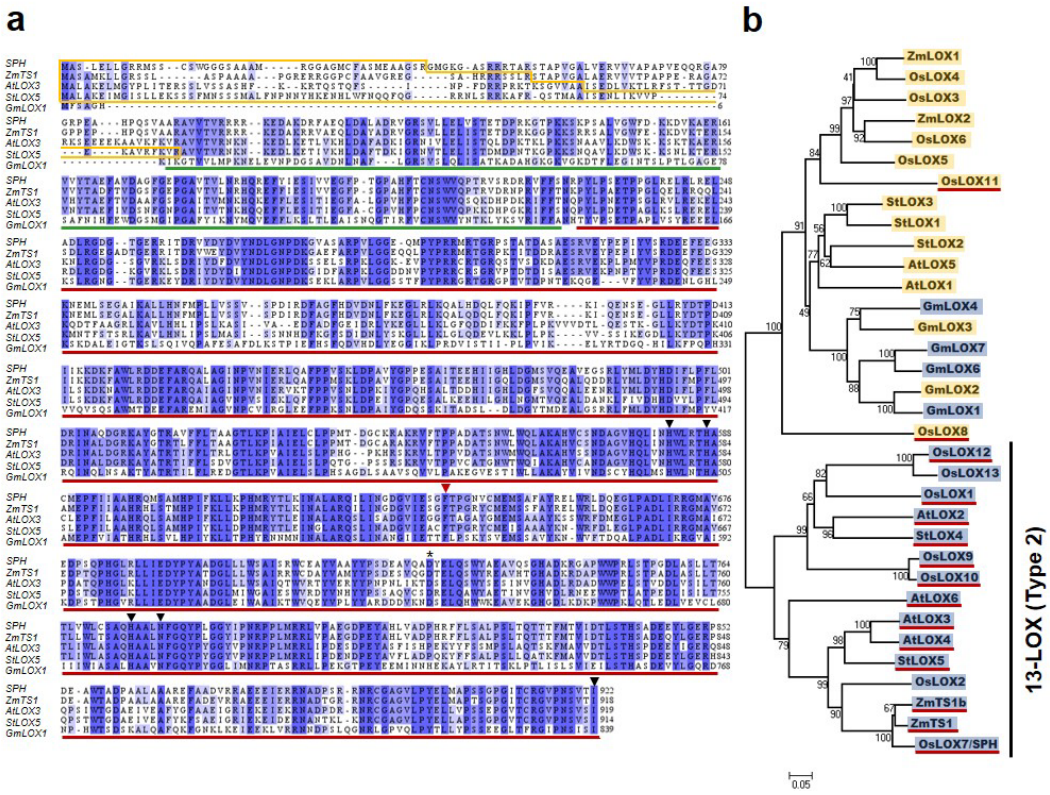

Figure 1-10. Multiple sequence alignment and phylogenetic analysis of LOXs. **a** Multiple amino acid sequence alignment of LOXs in various species. Predicted cTPs are indicated by yellow boxes and predicted PLAT/LH2 and lipoxygenase domains are underlined with green and red bold lines, respectively. Asterisk indicates the amino acid residue that was altered by the missense mutation in *sph*. The black arrowheads mark the five conserved residues necessary for iron binding. The red arrowhead indicates the conserved phenylalanine residue in 13-LOX. **b** Phylogenetic analysis of LOX proteins in various species. The bar indicates the relative divergence of the sequences analyzed, and bootstrap values are represented on each branching position. The blue and yellow boxes indicate 13-LOX and 9-LOX, respectively. LOXs predicted to have cTP are underlined in red. Os, *Oryza sativa*; At, *Arabidopsis thaliana*; St, *Solanum tuberosum*; Zm, *Zea mays*; Gm, *Glycine max*.

Expression pattern of *SPH*

To investigate the expression pattern of *SPH* gene, total RNA was extracted from various organs of HSC and conducted quantitative Real time PCR (qRT-PCR) analysis. *SPH* was expressed in all organs examined, with relatively higher expression levels in roots and stems than those of leaves and spikelets (Fig. 1-11b). Similarly, the expression of the transgenic plants conferring GUS reporter gene fused with 5'-upstream promotor region of *SPH* were observed in various organs. GUS signals from *proSPH*:GUS were detected in nodes, leaf veins, roots, anthers, and the marginal region of lemma (mrl) (Fig. 1-11c-i). Interestingly, GUS signal was concentrated in inner tissue of the mrl in which hull splitting occurred.

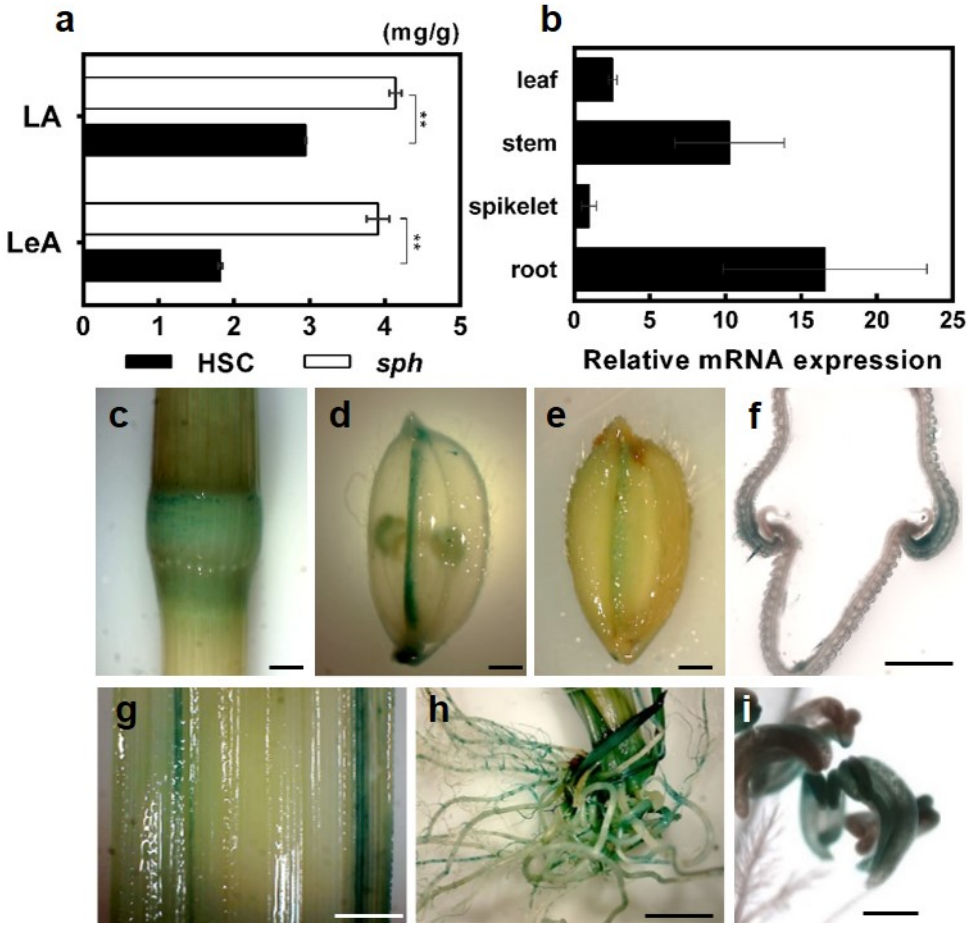

Figure 1-11. Quantitative analysis of fatty acids and expression analysis of *SPH*. **a** Quantitative analysis of LA (linoleic acid) and LeA (linolenic acid) contents in spikelets. **b** qRT-PCR analysis of *SPH* expression (normalized to *ACTIN*) in leaf, stem, spikelet, and root tissue. **c-j** β-Glucuronidase (GUS) expression pattern in various organs in the *proSPH*:*GUS* transgenic plant (**c**, node; **d**, spikelet; **e**, grain [20 DAF]; **f**, marginal region of the lemma [mrl]; **g**, leaf; **h**, root [20 day after germination]; **i**, anther). Error bars indicate ± s.d. of three replicates. Asterisks indicate significant difference, as determined by a two-tailed Student's *t*-test (*, $p < 0.05$; **, $p < 0.01$). Scale bar = 1 mm (**c**-**e**), Scale bar = 2 mm (**g**-**h**), Scale bar = 0.5 mm (**f**, **i**).

DISCUSSION

A mutant used in this study was firstly found in Seoul National University Farm in 1990's. The *split-hull* mutant ('74723') contained a single recessive gene and was associated with hull splitting in rice spikelets (Lee et al. 2004). This mutant line has been studied repeatedly in this study and we confirmed that the phenotypic expression in spiklelets was stable. Ratio of split-hull in the *sph* mutant varied along individuals from 34% to 58% with the average of ~47% suggesting that expressivity might be involved in this trait (Miko 2008). In particular, most of split hull grains were observed in secondary rachis branch in panicle of *sph* mutant (Lee 2012). These imply that the split hull phenotype expressivity is associated with the variation of each of spikelets in the panicle, such as hull size and grain filling.

In this study, we characterized the *sph* mutant and performed map-based cloning to isolate the gene governing the mutant phenotype. Through the characterization of physical and morphological properties of grain, several morphological differences between wild type and *sph* mutant were observed. First, grains of *sph* mutants showed weak mechanical strength of hull. Grains of *sph* mutantwere easily dehulled with low mechanical dehulling stress. In cell wall composition, amount of lignin in hull was significantly lower in *sph* mutant than in wild type. It is previously reported that lignin plays an important role in plant tissue rigidity (Pedersen et al. 2005). The

reduction of lemma lignification is observed in naked oat which has thinner and less grid lemma and free-threshing character (Ougham et al. 1996). These results easily lead to the inference that the reduced lignin content affects the mechanical strength of the hull, resulting in splitting and tearing of hull in the *sph* mutant. Second, the lemma width of *sph* mutant was smaller than that of wild type. Compared with wild type, *sph* mutant showed significant reduction of lemma width with no differences in other parts of hull. These results revealed that reduction of lemma width in the mutant was a major determinant for the *sph* mutant phenotype. Third, the thickness of dehulled seeds (brown rice) of *sph* mutant varied depending on the existence of hull splitting. There was no significant difference in seed length and width between *sph*-nor and *sph*-sh seeds, whereas *sph*-sh seeds were thicker than those of the wild type and *sph*-nor seeds. Possibly different grain filling rate in each spikelet could explain the difference. Because the size and shape of caryopsis are restricted by hull size (Takeda and Takahashi 1970; IRRI 1991), each hull receives different repulsive force depending on the degree of grain filling. Therefore, we concluded that the reason of hull splitting phenotype in *sph* mutant is imbalance between hull size (storage capacity) and grain filling (source supplying capacity) in condition of weak hull phenotype. Unfortunately, there was no direct evidence on the morphological difference in interlocking part of lemma and palea between wild type and *sph* mutant in this study. However, the expression of *SPH* was specifically detected in the inner joint part of the lemma. This expression pattern implies that delicate changes that we

couldn’t discover in this investigation may affect the hull splitting phenotype. Further studies are required to reveal the relation between hull splitting and the expression pattern.

SPH encoding a type-2 13-LOX was isolated by map based cloning approach. LOXs catalyze the deoxygenation of poly unsaturated fatty acids (PUFAs) containing a (Z,Z)-1,4-pentadien system, such as LA and LeA (Siedow 1991). In quantitative analysis of fatty acids, *sph* mutant contained higher levels of both LA and LeA in spikelets than wild type. These results can be interpreted that the mutation occurring in the LOX catalytic domain of *SPH* might cause a reduction in oxygenation activity in this mutant, resulting in an increase in the levels of these underutilized substrates. Gene expression analysis showed that *SPH* was expressed in various organs, including leaf, node, pollen, mrl, and root. The *sph* mutant phenotypes such as increased CL and reduced SSR may be related to expression of *SPH* in internode and pollen. The expression level of this gene was high in root, suggesting that the existence of *SPH* functions in root growth and development or other physiological responses. Further studies are required to examine the role of *SPH* in root and other plant parts.

LOXs are responsible for the first reaction of LOX pathway which synthesize various oxylipins, such as divinyl ethers, epoxy hydroxy fatty acid, leaf aldehydes, leaf alcohols, ketols, and jasmonic acid (JA). Oxylipins function as potent bio-regulators involved in plant growth and development, signaling cascades,

senescence, organogenesis, and the maintenance of homeostasis (Grechkin 1998). The roles of LOXs in various responses have been investigated in rice, such as responses to wounding and insect attack, seed longevity and storage, and the production of stale flavors (Ohta et al. 1991; Suzuki et al. 1999b; Zhou et al. 2014; Huang et al. 2014). In previous studies of *SPH* orthologs, loss of function mutants showed defective floral organ phenotypes. In maize, *TASSELSEED1* (*TS1*) plays a role in regulating pistil abortion to complete staminate inflorescence. The *ts1* mutant shows conversion of tassel inflorescence from staminate to pistillate (Acosta et al. 2009). Likewise, the Arabidopsis *lox3lox4* double mutant is male sterile and taller than the wild type (Caldelari et al. 2011). All of these defects caused by loss of function on LOXs are recovered by treatment with exogenous JA. Furthermore, there are several results that lignin biosynthesis related gene positively induced by treatment with Methyl jasmonate (Salzman et al. 2005a; Pauwels et al. 2008). The *sph* mutant also showed reduced lignin content and SSR, increased CL, abnormal spikelets, and hull splitting phenotype, although it is a little different defective phenotype of floral organ compared with that generated in orthologs. Taken together, we speculate that the *sph* mutant phenotype is caused by effect of downstream processes affected by reduced LOX catalysis, such as JA biosynthesis and lignin biosynthesis of which related genes are regulated by JA content, but further studies are needed to reveal the underlying molecular mechanism.

Rice hull plays an important role in protecting reproductive organs before

fertilization, as well as developing the seeds during the grain filling stage. However, this organ should be removed by dehulling (or dehusking) process in order to consume caryopsis inside hull. During dehulling process, rice grains are subjected to mechanical stresses causing the appearance of broken rice. Broken rice appearance rate can be determined by the dimension and the strength of hull as well as caryopsis characters such as fissures, chalkiness, and immaturity (Buggenhout et al. 2013). In other cereal crops such as wheat, barley, and oat, a number of genetics and breeding programs on some naked grains and their associated genes have been conducted to develop easy dehulling (or free-threshing) cultivars (Taketa et al. 2008; Sormacheva et al. 2014; Ubert et al. 2017). However, no study on dehulling trait which might be beneficial to develop a new cultivar has been reported in rice. Low mechanical dehulling stress which is wide roller distance will reduce rice caryopsis break that causes rice yield loss (Swamy and Bhattacharya 1979). It is reported that *indica* cultivars, long-slender grain, are more susceptible to mechanical stress, resulting in high levels of broken rice compared to *japonica* cultivars (Buggenhout et al. 2013). High dehulling efficiency with low dehulling stress is further required in specialty rice cultivars that produce easy-breaking grain character and brown rice cultivars, such as giant embryo, sugary, and colored rice (Koh et al. 1993b; Koh and Heu 1994). Because, in brown rice cultivars, the levels of broken rice during dehulling process directly affects to yield loss, high dehulling efficiency of brown rice cultivars means high milling rate. Thus, the application of the *sph* mutant may

facilitate the breeding of high dehulling efficiency rice for reducing yield loss.

CHAPTER Ⅱ

Identification of the *LARGE EMBYRO* (*LE*) Gene Controlling Embryo Size in Rice

ABSTRACT

Rice embryo accounts only for 2-3% of the total kernel mass but is a good source of various nutrients and non-nutrients for human health. Generally, embryo size shows positive correlation with the contents of various nutrients and bioactive sources. Therefore, giant embryo mutants are very useful breeding material to improve nutritional quality of rice. Three giant embryo mutants (*le*, *ge*, and ge^s) showing variation in embryo size were characterized and genetically analyzed to reveal their mutual allelism and to check novelty of loci. The *ge* mutant was allelic to ge^s mutant in allelism test, and both mutants had its own nucleotide substitution causing nonsynonymous mutation in the 2nd exon of *GIANT EMBRYO* (*GE*). On the contrary, the *LARGE EMBRYO* (*LE*) mutant was not allelic to *ge* and ge^s, and thus considered that *LE* is a novel gene controlling embryo size. The *le* mutant showed mild enlargement in embryo size caused by increase of scutellar parenchyma cells size. *LE* encodes C3HC4-type RING finger protein and was shown relatively high expression in a late seed developing stage. The knock-down transgenic plants

produce enlarged embryo grain, which demonstrates *LE* gene is participated in regulation of embryo morphology. These results provide the basis of new regulation mechanism in controlling embryo size and suggest that *le* mutant will contribute to the development of new giant embryo cultivars.

Keyword: Rice, Large embryo, Giant embryo, C3HC4 RING finger protein, Nutritional quality

INTRODUCTION

With ever-increasing demand for high quality rice, researches and efforts to improve quality of rice have been carried out more actively (Fitzgerald et al. 2009). Mature rice embryo typically occupies 2-3% of the total kernel mass, but accumulates various nutrients such as proteins, lipids, vitamins, minerals, and phytochemicals. Embryo accounts for more than 95% of total tocopherols, one-third of the oil content, and 98% albumin of the rice grain (Gopala Krishna et al. 1984; Tanaka et al. 1977). These high nutritional value of embryo makes it popular to use byproduct (bran), brown rice, and polished embryonic rice.

Breeding efforts to improve nutritional quality of rice were started from induction and isolation of mutants. Various mutants responsible for the embryo/endosperm size balance have been reported, such as endospermless mutants, embryoless mutants, reduced embryo mutants, and giant embryo mutants in rice (Satoh and Omura 1981b; Hong et al. 1995a). Using these breeding material, numerous giant embryo cultivars have been reported to date (Maeda et al. 2001; Takahashi et al. 2009; Hong et al. 2012b; Han et al. 2012b), and giant embryo lines generally contain more protein, lipid, essential amino acid, vitamins (V_{B1} V_{B2} and V_E), minerals (Ca, Fe, Mg, K and P) and bioactive sources (GABA and γ-oryzanol) (Koh et al. 1993a; Zhang et al. 2005; Jeng et al. 2012; Kim et al. 2013).

To date, only two genes related to the enlargement of embryo size have been

cloned. *GE* locus was mapped on chromosome 7 (Satoh and Iwata 1990; Koh et al. 1996). This *GE* gene encoding cytochrome p450 protein, CYP78A13, was cloned by Nagasawa et al. (2013), and they revealed that *GE* functions in the embryo to control cell size and in the endosperm to regulate cell death via ROS signaling, resulting in large embryo and small endosperm with loss of function in *GE*, but small embryo and enlarged endosperm with overexpression of *GE*. In addition, Yang et al. (2013) reported that *GE* gene also plays critical role in SAM maintenance. In maize, reduced expression of *ZmGE2* which was caused by insertion of transposable element leads to increase in embryo to endosperm ratio (EER). *ZmGE2* encodes cytochrome p450 protein, and overexpression of *OsGE* in maize induced decrease of EER, suggesting that cytochrome p450 plays an important role in regulating embryo size and the mechanism of EER determination is evolutionarily conserved in rice and maize (Zhang et al. 2012). Another embryo size related gene, *GOLIATH* (*GO*), was mapped on chromosome 3 (Taramino et al. 2003). Unlike *ge* mutant, enlarged embryo phenotype of *go* mutant was caused by increased cell number. The *plastochron3* (*pla3*) mutant exhibits pleiotropic phenotypes including enlarged embryo, seed vivipary, defects in SAM maintenance, and aberrant leaf morphology. *PLA3* encodes glutamate carboxypeptidase and is allelic to *GO* (Kawakatsu et al. 2009). Recently, new giant embryo breeding materials were reported that they showed enlarged embryo and increase of triacylglycerol compared with wild type. The new locus was not allelic to *GE*, and mapped on different region of *GO* in

chromosome 3 (Sakata et al. 2016).

In this study, we performed allelism test among three giant embryo mutants (Kim et al. 1991) and identified *LARGE EMABRYO* (*LE*) gene. Since ge^m is not allelic to previously reported genes (*GE* or *GO*), we changed the mutant name and locus nomenclature from *giant embryo-moderate* (ge^m) to *large embryo* (*le*) to prevent confusion with *GE*. The *le* mutant had mildly enlarged embryo and showed no defects in growth and germination. In addition, seonong17, a cultivar derived from *le* mutant, showed high hypolipidemic effect, body fat-lowering effect, and high antioxidant capacity (Chung et al. 2014b; Chung et al. 2016a). Therefore, *le* mutant could be valuable for breeding of speciality rice cultivar.

MATERIALS AND METHODS

Plant materials

Three giant embryo mutants were named as *le*, *ge*, and ge^s, in ascending order of embryo size. Hwacheong (HC), a *japonica* cultivar, was used as the wild type when comparing phenotype with mutants. The F_2 seeds derived from a cross between *le* mutant and HC was used to calculate the segregation ratio. Map-based cloning was conducted by using F_2 and F_3 population derived from a cross between the *le* mutant and Hangangchal1 (a Korean *Tongil*-type cultivar). All plant materials were grown at the Experimental Farm Seoul National University (Suwon, Korea) under normal cultivation conditions.

Phenotypic analysis

The dimensions of the grains and brown rice were measured from microscopic images with HD'MEASURE software (HANA Vision, Korea). To measure ENW, EMW, and EER, husked seeds (14% water content) were dissected into embryos and endosperms, and each part was separately weighed using an electronic balance (CAS, USA). Agronomic traits such as DTH, CL, PL, PN, SPP, and SF were also measured to compare morphological differences among wild type and giant embryo mutants.

Histological analysis

Seeds of HC and giant embryo mutants at the 20 Days after pollination (DAP) were fixed in formalin-acetic acid-alcohol (FAA) fixative buffer (3.7% formaldehyde, 5% acetic acid, 50% ethanol) for 24 hrs at 4°C. The seeds were dehydrated by soaking them for 2 hrs each in a graduated ethanol solution of increasing concentration. After final dehydration with 100% ethanol, the seeds were cleaned by soaking in cleaning solution series that ethanol was gradually substituted by histoclear, followed by soaking in 100% histoclear solution overnight. For paraffin infiltration, Paraplast® (Sigma, USA) was gradually added to histoclear solution at 60°C. Finally, the seed samples were maintained in 100% melted paraffin for 24 hrs at 60°C. The paraffin-infiltrated samples were embedded in an embed block and cut into 10 μm sections with an HM 340 E Rotary Microtome (Microm Lab, Germany). The sections were stained with 1% safranin O solution (1% safranin O, 30% ethanol) and examined by Microscope CX31 (Olympus, Japan).

Quantification of GABA content

50 mg of finely ground brown rice powder was homogenized with 1 ml of 0.01 N HCl prepared in 25% acetonitrile, and then centrifuged at 13,000 rpm for 3 min. After filtered with 0.2 um syringe filter, the clear supernatant was derivatized by using EZ: Faast kit (Phenomenex, USA) followed by detection through gas chromatography. A GC-2010 gas chromatograph (GC-2010, Japan) equipped with a

flame ionization detector (FID) was used with a ZB-5(30 m x 0.25 mm, 0.25 um) capillary column. Each sample was tested four times.

Allelism test and sequence analysis

F_1 and F_2 seeds derived from reciprocal crosses among HC, and three mutants were used for genetic analysis. F_2 seeds of each cross combination were classified according to the embryo size, and x^2 (chi-square) test was performed. Two overlapping DNA fragments including ORF of *GE* gene (Nagasawa et al. 2013) were amplified by PCR. The PCR products were sequenced with an ABI Prism 3730 XL DNA Analyzer (PE Applied Biosystems, USA). The sequences of HC and three giant embryo mutants were aligned using CodonCode Aligner software (CodonCode Cor., USA) and analyzed. Co-segregation test conducted to detected SNP using CAPS and dCAPS primer (Table 2-1)

Map-based cloning of *LE*

20 mutant type plants and 20 wild type plants were selected from F_2 population derived from *le* mutant/Hangangchal1 to make DNA bulks. BSA was performed by screening 66 STS markers (Michelmore et al. 1991; Chin et al. 2007). For fine mapping, 397 F_2 plants and 857 F_3 plants were used, and seven STS markers were newly designed with primer 3 version 0.4.0 (http://bioinfo.ut.ee/primer3-0.4.0) based on the DNA sequence differences between *indica* and *japonica* rice

subspecies (https://blast.ncbi.nlm.nih.gov and http://gramene.org). The information of designed and used markers are listed in Table 2-1.

Candidate gene analysis

To identify the variation in the candidate genes, DNA fragments of the genes were amplified using designed primers (Table 2-1). PCR products derived from HC and *le* mutant were purified using a Gel & PCR Purification kit (Inclone, Korea) and cloned into pGEM-T Easy Vector (Promega, USA), followed by transformation into *E. coli* strain DH5α. Transformed plasmid which were purified by Plasmid mini prep kit (Inclone, Korea) were sequenced with an ABI Prism 3730 XL DNA Analyzer (PE Applied Biosystems, USA) and aligned using CodonCode Aligner software (CodonCode Corporation, USA). Co-segregation test was conducted to detect one nucleotide deletion point using dCAPS marker (Table 2-1).

Multiple sequence alignment

The amino acid sequences showing high similarity to LE were downloaded from the Universal Protein Resource (UniProt, http://www.uniprot.org). Multiple sequence alignment was carried out using Probcons, and background color shading was applied with Jalview using the % identity scheme. The information of the protein sequences used in this study are listed in Table 2-2. Transmembrane motif was predicted using TMHMM server v. 2.0 (http://www.cbs.dtu.dk/services/TMHMM/).

RNA extraction and qRT-PCR analysis

Total RNA was extracted from leaf, stem, root, and seed (5 DAP and 20 DAP) tissues using Hybrid-R™ RNA purification kit (GeneAll, Korea), and the extracted RNAs were treated with RNase-free Recombinant DNase I (Takara Bio, Japan) to eliminate genomic DNA contamination. First-strand cDNA was synthesized using M-MLV reverse transcriptase (Promega, USA). qRT-PCR was performed using SYBR premix ExTaq (Takara, Japan) on a CFX96™ Real-Time PCR system (Bio-Rad, USA) following the manufacturer's instructions. Expression of *LE* was normalized to those of *UBIQUITIN5*. The primers for qRT-PCR are listed in Table 2-1.

GUS staining

GUS staining was carried out as previously described (Jefferson et al. 1987). The GUS staining solution was vacuum-infiltrated into various organ samples for 10 min. The samples were incubated overnight at 37°C in staining solution, followed by incubation in 90% ethanol overnight at room temperature to bleach the chlorophyll in the samples.

Vector construction and transformation

To generate RNAi and *LE promoter*::GUS transgenic plant, the promoter region (-2135 to -1 bp) and 3'UTR (+6925 to +7215 bp) of *LE* was amplified by PCR, and each PCR product was cloned into pHGWFS7 and pH7GWIWG2(II), respectively, using Gateway® BP and LR Clonase™ II enzyme mixes (Invitrogen, USA). The final constructs were introduced into Dongjin through transformation with *Agrobacterium* strain LBA4404. Transformation was carried out using a previously published *Agrobacterium*-mediated transformation method (Nishimura et al. 2007) with slight modifications. Primers used for cloning DNA fragment are listed in Table 2-1.

Statistical analysis

Statistical analysis of phenotypic data and expression data was conducted using IBM SPSS Statistics software version 24 (IBM, USA). The segregation ratios of F_2 seeds derived from reciprocal crosses among three mutants were statistically analyzed for deviation from the expected Mendelian segregation ratio (3:1 or 9:3:4) by x^2 test using Excel 2013 (Microsoft Corp., USA).

Table 2-1. Information of the primers used in this study

Primer name	Purpose	Forward primer (5'→'3')	Reverse primer (5'→3')	Note
CAPSge	Segregation test	CCCTACATCCAGTCCATCGT	ATCGCCCACATGTTCACC	CAPS (SphⅠ)
dCAPSgesX	Segregation test	ACCCGCCGGGCCCACTCCTGTCGT	GTCCTCCCCCTCCGAGAAG	dCAPS (XcmⅠ)
dCAPSle	Segregation test	TTATCTTTCAGGTATGGAGGCTCCAAGAAG	AAGCTGAGCGACCTAAATGG	dCAPS (HindⅢ)
M1	Mapping	GGTAATCATCAGCGTTGTGAGA	TTAGCTTTGCCCCATGTCTACT	InDel
M2	Mapping	CCGTGTCAATTGGTACTTGG	TATCCGGCCTCTGCAATAAG	InDel
M3	Mapping	AAGTTGCAACGAAAAAGACAAA	CACCTACGGCCTAGCTTTGA	InDel
M4	Mapping	GAAAAACTCGGAAGAAAAGCAA	GGTTTAAATTGGGTTCAGCAA	InDel
M6	Mapping	ATATCCGGTTCCACCTGTCA	CAGGGCCTACCCAGCTTATAC	InDel
M7	Mapping	TGTCTCACCAATATAAGGTGTCC	TCCATCCGTTTATGGGATTC	InDel
M5	Mapping	TCCGATTGACACAGCTCTAACT	GGGATGGAGTGGAGCAGTAA	InDel
RM01350	Mapping	GAGGAAATTCGCCCTAGTAG	AAGAAAGCTCTGCTCCATGC	SSR
S03128	Mapping	TGATGCAAAGACTGCGAAAC	GGGAGTAGTGCGCTTTTGAT	InDel
GE-T1	*GE* gene sequencing	TTGGAGTGGCAAAATGGTCTA	TGTCCGTCCCTCTAAAGATCA	-
GE-T2	*GE* gene sequencing	CGACATGATCGCTGTTCTTT	CTGACAGCCAACTGGAGAAAT	-
LE1	LE gene sequencing	TAAAACGCAACGCACAGAAG	TTCAAAGGCCAGAAGAGGAA	-
LE2	LE gene sequencing	TGCTTATTGCGTTTGAGCTG	AAAATGCCAATGAGCCTGAC	-
LE3	LE gene sequencing	ATAGGTTGGGCCCTCTCATC	GTCATGTGCAAGGAAGCAAA	-
LE4	LE gene sequencing	GCACTTTTGGGTTGCAATTT	CTAGCCTCCCCAGGATTAGG	-
LE5	LE gene sequencing	CAGGTGATGTTGGTGCTTTG	GCCTTTCAAATTCCTGCTTG	-
LE6	LE gene sequencing	GCCTAAGAGGGATCTTGCAG	ATGCACAAAAGCAACCCTTC	-
qRT-LE	qRT-PCR	CAGCCTACTCCTGGTGGATT	AATGGCAAGGAGCCCAAT	-
LE-RNAi	LE RNAi transgenic line	AAAAAGCAGGCTAACGCATGCCCGTATATGAT	AGAAAGCTGGGTGGAGCATCTATCGATCACCAA	-
LE-GUS	LE GUS transgenic line	AAAAAGCAGGCTGAACGGTTGTCAGCCATTTT	AGAAAGCTGGGTCCCTCACCTCCTCACCGCGC	-

Table 2-2. Information of LE orthologs used in multiple sequence analysis

Organism	Nomenclature in this study	gene ID	Sequence length	UniProtKB accession
Oryza sativa	OS03g0706900/LE(Os)	*OS03g0706900*	473	Q10E70
Triticum aestivum	M1FYS2(Ta)	-	473	M1FYS
Hordeum vulgare	F2D8D3(Hv)	*HORVU4Hr1G007020*	473	F2D8D3
Zea mays	Zm00001d033674(Zm)	*Zm00001d033674*	473	B6T9X2
Arabidopsis thaliana	AT1G73950(At)	*AT1G73950*	466	F4HS21
Brassica rapa	Bra015952(Br)	*Bra015952*	467	M4DHH5
Glycine max	LOC100791390 (Gm)	*GLYMA17G13040*	466	I1MUG1

RESULTS

Characterization of three giant embryo mutants

Three giant embryo mutants were induced by treatment of *N*-methyl-*N*-nitrosourea (MNU) on fertilized egg cell of Hwacheong (HC), a *japonica* cultivar (Kim et al. 1991). These giant embryo mutants were previously characterized by (Lee 2013). All of these mutants showed enlarged embryo phenotype compared with wild type (HC) and represented difference in degree of enlargement among each mutants. According to embryo size from small to large, three giant embryo mutants were named *large embryo* (*le*), *ge*, and ge^s, respectively (Fig. 2-1 and Fig. 2-2d). In comparison of grain characteristics, there was no difference in the width of brown rice, but ge^s mutant indicated significant increase of the length of brown rice and length-width ratio compared with wild type (Fig. 2-2a-c). We evaluated the altered embryo size as the ratio of embryo to endosperm by measuring the weight of dissected embryo and endosperm. Giant embryo mutants showed significantly reduced thousand grain weight (TGW) and endosperm weight (ENW), but increased embryo weight (EMW) compared with those of wild type (Fig. 2-2e-g). As the EER gradually increased in the order of *le*, *ge*, and ge^s mutant, the GABA content also increased according to increase of embryo size (Fig. 2-2h). Enlarged embryo phenotype was caused by a conspicuous enlargement of scutellar parenchyma cell size in all mutants (Fig. 2-2i, n-q).

Figure 2-1. The phenotype of grain and embryo of HC and three giant embryo mutants. From left to right; HC, *le*, *ge* and *ge*^{s} mutant. Scale bar = 2 mm.

Although three giant embryo mutants did not perform serious defects of shoot and radicle differentiation, shoot size of *ge* and *ge*^{s} were slightly reduced compared to *le* mutant and wild type (Fig. 2-2j-m). The *le* mutant indicated significant differences in other agronomic traits such as reduced CL, GW, GL, and LWR compared with wild type (Table 2-3).

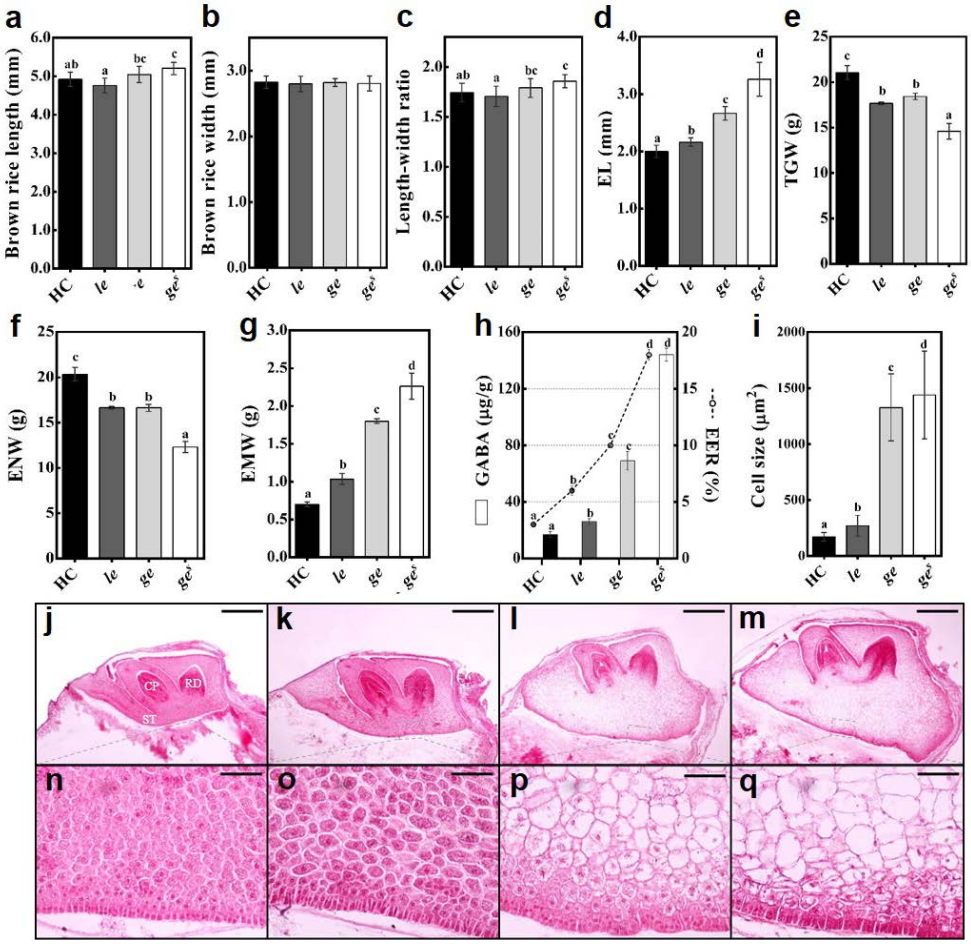

Figure 2-2. Characterization of grain and embryo related traits of wild type and giant embryo mutants. **a-i** Evaluation of brown rice and embryo related traits. Dimension of seed (**a-c**); EL, embryo length (**d**); TGW, thousand grain (brown rice) weight (**e**); ENW, endosperm weight (1000 seeds) (**f**); EMW, embryo weight (1000 seeds) (**g**); GABA content and EER, embryo to endosperm ratio (**h**); Cell size of scutellar pharenchyma (**i**). **j-q** Longitudinal sections of embryo at 20 DAP: wild type (**j** and **n**), *le* (**k** and **o**), *ge* (**l** and **p**), and *ge*^{s} (**m** and **q**). CP, coleoptiles; RD, radicle; ST, scutellum (**n-q**). The means followed by superscript letters are significantly different ($p < 0.05$, ANOVA) according to Duncan test. Error bars indicate ± s.d. of replicates. Scale bar = 0.5 mm (**j-m**), Scale bar = 50 μm (**n-q**).

Table 2-3. Agronomic traits of HC, *le*, *ge* and *ge*^{s} mutant

	DTH (day)	**CL** (cm)	**PL** (cm)	**PN** (No.)	**SPP** (No.)	**SF** (%)	**GW** (mm)	**GL** (mm)	**LWR**
HC	115	86.4^{b}	18.5^{ab}	12	95	93.3	3.56^{bc}	5.95^{b}	1.77^{b}
le	114	77.0^{a}	18.7^{b}	12	101	91.1	3.28^{a}	5.57^{a}	1.70^{a}
ge	118	88.9^{b}	17.6^{a}	14	100	92.4	3.41^{c}	5.98^{b}	1.76^{b}
***ge*^{s}**	113	89.0^{b}	19.1^{b}	13	105	94.9	3.34^{ab}	5.91^{b}	1.77^{b}

DTH, days to heading; CL, culm length; PL, panicle length; PN, panicle number; SPP, spikelet per panicle; SF, spikelet fertility; GL, grain length; GW, grain width; LWR, length-width ratio. The means followed by lowercase letters are significantly different ($p < 0.05$, ANOVA) according to Duncan test.

Genetic analysis of giant embryo mutants

To confirm allelism and heritable form of genes responsible for enlarged embryo phenotype in three mutants, we investigated F_2 seeds segregation ratio of each cross derived from reciprocal crosses among HC, *le*, *ge*, and *ge*^{s} mutants (Lee 2013). F_2 seeds that were generated from reciprocal crosses between each mutants and HC segregated in a 3 (normal embryo-type): 1 (enlarge embryo-type) ratio, indicating that each enlarged embryo mutant caused by a mutation in single recessive gene, respectively (Table 2-4). Koh et al. (1996) mapped *ge*^{s} locus on chromosome 7, and Nagasawa et al. (2013) isolated *GE* gene from the mapping region. Therefore, we inferred that enlarged embryo phenotype of *ge*^{s} mutant was induced by mutation on *GE* gene. In the reciprocal crosses between *ge* and *ge*^{s}, The EL of F_1 seeds were

increased and all F_2 seeds showed enlarged embryo type, indicating that the locus in *ge* is identical to *ge*^{s} (Table 2-4). On the other hand, F_2 seeds derived from reciprocal crosses between *le* mutant and other two giant embryo mutants were segregated into three types of seeds, normal type, *le* type, and *ge* (*ge* or *ge*^{s}) type depending on the embryo size. All F_2 segregation ratios for normal type: *le* type: giant embryo type fitted the 9:3:4 ratio, suggesting that enlarged embryo phenotype of *le* was not allelic to *GE* (Table 2-4).

Table 2-4. Segregation of F_2 seeds from the reciprocal crosses among HC and three giant embryo mutants

Cross combination	F_1 EL (mm)	Type of embryo				Expected ratio	x^2	*p*-value
		wild	*le*	*ge*	*ge*^{s}			
HC/*le*	2.10[a]	299	99	-	-	3:1	0	1
***le*/HC**		260	100	-	-	3:1	1.34	0.25
HC/*ge*	2.16[a]	348	-	134	-	3:1	1.87	0.17
***ge*/HC**		269	-	83	-	3:1	0.31	0.58
HC/*ge*^{s}	2.12[a]	246	-	-	76	3:1	0.27	0.61
***ge*^{s}/HC**		265	-	-	84	3:1	0.12	0.73
le*/*ge	2.15[a]	177	64	71	-	9:3:4	1.16	0.56
ge*/*le		145	48	63	-	9:3:4	0.02	0.99
***le*/*ge*^{s}**	2.21[a]	178	60	-	78	9:3:4	0.02	0.99
ge*^{s}/*le		160	51	-	63	9:3:4	0.67	0.72
ge*^{s}/*ge	3.12[b]	-	-	296	117	3:1	2.27	0.13
***ge*/*ge*^{s}**		-	-	106	45	3:1	1.61	0.2

The means followed by superscript letters are significantly different ($p < 0.05$, ANOVA) according to Duncan test. EL, embryo length.

Sequencing analysis of *GE* locus in three giant embryo mutants

In sequence comparison of *GE* (*Os07g0603700*) locus, we found G 1169 A base change causing a Arg 390 His amino acid substitution and G 1199 T base change causing a Trp 400 Leu amino acid substitution in *GE* locus of *ge* and ge^s, respectively. These mutations were co-segregated with enlarged embryo phenotype in F_2 seeds generated from crosses between HC and mutants (*ge* and ge^s). However, there was no nucleotide change in *GE* locus of *le* mutant. In addition, we could not find any variation in *PLA3/GO* locus of *le* mutant. In conclusion, embryo size of *ge* and ge^s were affected by mutation generated in *GE*, while those of *le* was controlled by other gene. These results were consistent with the previous allelism test.

Map-based cloning of *LE* gene

To isolate the gene related to enlarged embryo phenotype in *le* mutant, we conducted map-based cloning using F_2 and F_3 population derived from cross between *le* mutant and Hangangchal1. Through BSA, *LE* gene is showed to link with insert and deletion (InDel) marker S03128 on chromosome 3. Sakata et al. (2016) reported that new *giant embryo* (MGE8 and MGE14) locus mapped on the short arm of chromosome 3, but this region was far from our candidate region. To refine the position of *LE* locus, a series of InDel markers were newly developed based on the genome sequence differences between *indica* and *japonica* (http://www.ncbi.nlm.nih.gov/), and *LE* gene was finally mapped within an

approximately 52-kb region between M7 and M5 (Fig. 2-3a). Three predicted ORFs were located in this candidate region (Fig. 2-3b). In order to identify the best candidate for *LE*, we sequenced three ORFs in HC and *le* mutant and one nucleotide deletion was identified in the 12^{th} exon of *OS03G0706900* encoding C3HC4-type RING finger protein (Fig. 2-3c). The deletion occurred in the 1202^{th} ORF nucleotide (C 1202 del) is expected to substitute the 401^{th} amino acid, alanine, for a valine followed by a frameshift terminating after 82 aberrant amino acids (Fig. 2-3d). We developed dCAPS marker for genotyping of the mutant sequence variation. The result of dCAPS genotyping to F_2 individuals whose phenotype were determined by F_3 seed type revealed that the large embryo phenotype was co-segregated with the one nucleotide deletion, supporting that the one nucleotide deletion detected in *Os03g0706900* was responsible for the enlarged embryo phenotype (Fig. 2-3e). To determine whether the mutant variation is present as a natural variation in *Oryza sativa* genome, we confirmed genotype of 11 *Oryza sativa* (six *japonica*, two *tongil-type*, and four *indica*) and one *O.nivara* using dCAPS marker. None of these exhibited mutant variation (Fig. 2-3f). Therefore, we focused on *Os03g0706900* as a candidate for *LE* gene.

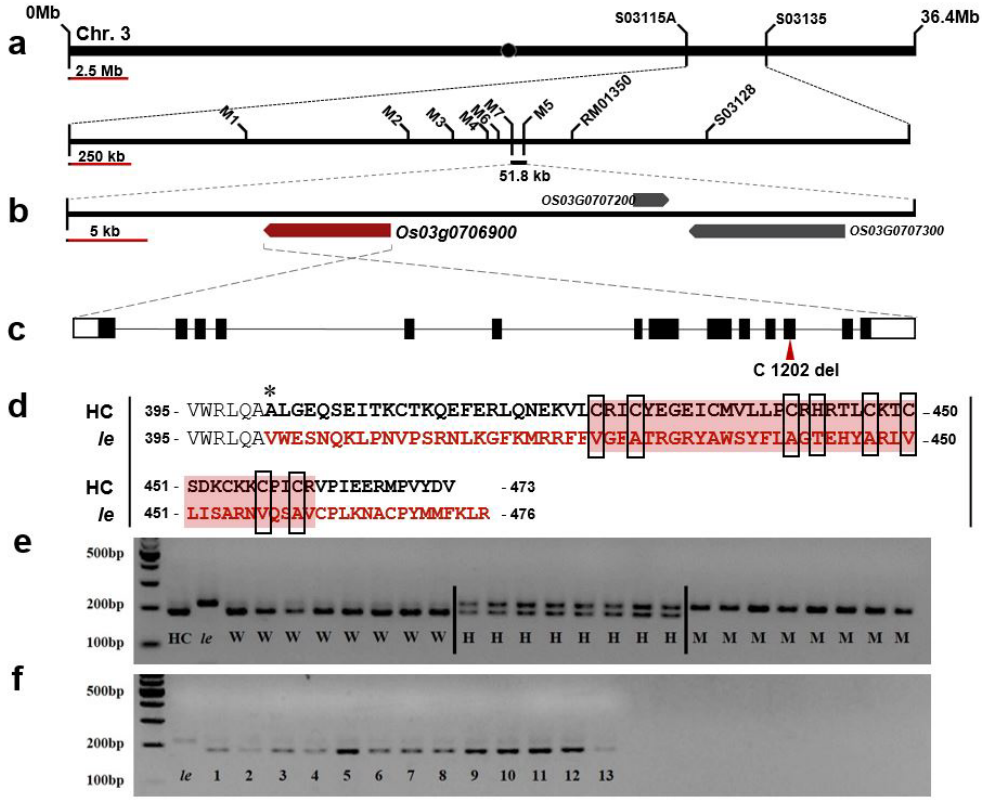

Figure 2-3. Map based cloning of the *LE* gene. **a** Schematic diagram of mapping of *LE* locus. **b** Candidate ORFs in mapped region. **c** *LE* gene structure and splicing pattern. The black lines, white solid boxes, and black boxes indicate intron, UTRs, and exons, respectively. The mutation position is marked with red arrow head. **d** Comparison of amino acid sequence of the frameshift region between the HC and *le* mutant. Asterisk represents the location of amino acid substitution caused by one base deletion in *le* mutant. Amino acids in the region of frameshift are indicated in red. Red background and black open boxes indicate amino acid sequences of C3HC4-type RING domain and conserved residues in the domain. **e** Co-segregation test on F_2 individuals. W, wild type F_2 progeny; H, hetero type F_2 progeny; M, mutant type F_2 progeny. **f** Co-segregation test on other cultivars and *O.nivara*. 1, Hwacheong; 2, Hwaseonchal, 3. Ilpum, 4. Unkwang, 5. Hapcheon, 6. Nipponbare, 7. Dasan, 8. Hangangchal 1ho, 9. IR36, 10. IR64, 11. IR56, 12. IR21015, 13. *O.nivara*.

Effect of *LE* knock-down on embryo size

To confirm that the defect of *LE* affects embryo size, we transformed an RNA interference (RNAi) construct that harbored a 291-bp specific mRNA fragment of *LE* into Dongjin via pH7GWIWG2(II) vector (Fig. 2-4a). Real-time quantitative PCR analysis showed that the expression level of *LE* was downregulated in RNAi transgenic plants compared with control Dongjin (Fig. 2-4b). The embryo size of RNAi transgenic plants was significantly increased compared with control (Fig. 2-4c, d). These results suggest that *LE* gene controls embryo size in rice.

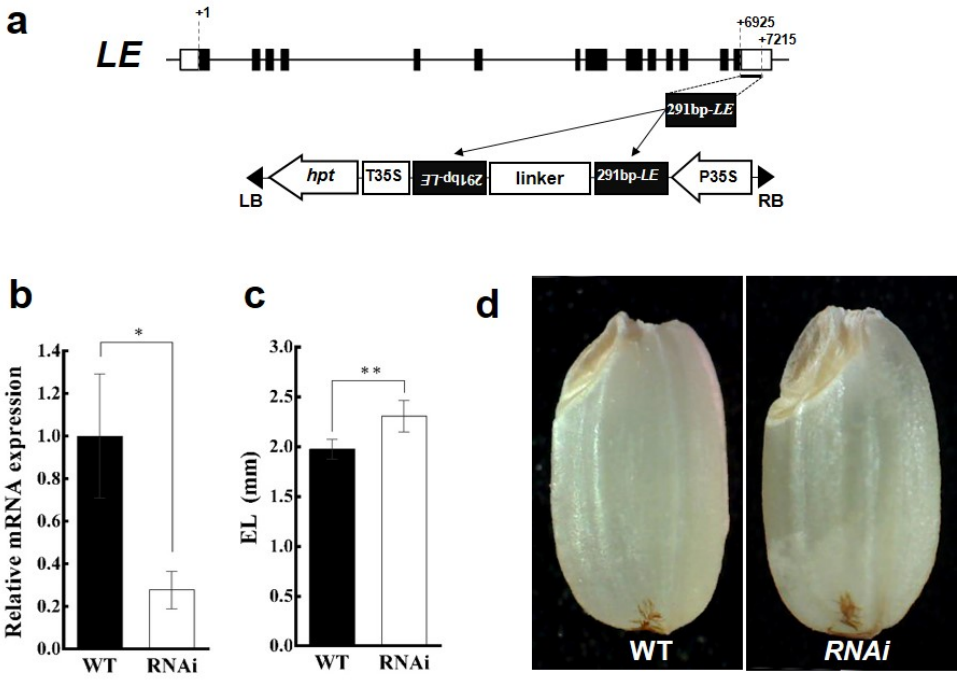

Figure 2-4. The embryo phenotype and *LE* expression of RNAi transgenic plant. **a** Structure of the RNAi construct. **b** Relative expression of *LE* (normalized to *UBIQUITIN*) in wild type and RNAi plants. **c** Comparison of embryo length between wild type Dongjin (WT) and RNAi plants. **d** Seed phenotype of RNAi plants. Error bars indicate ± s.d. of three replicates. Asterisks represent significant difference, as determined by a two-tailed Student's *t*-test (*, $p < 0.05$; **, $p < 0.01$). Scale bar = 1 mm.

LE gene encoding C3HC4-type RING domain protein

The *LE* gene is composed of 14 exons, with 13 intervening introns. The predicted protein consists of 473 amino acid residues with C3HC4-type RING domain in C-terminal, and seven transmembrane motifs (Fig. 2-5 and Fig. 2-6). Multiple

sequence alignment among orthologs of *LE* revealed that predicted transmembrane motifs and the consensus sequence of RING finger domain (Cys-X_2-Cys-X_{11}-Cys-X-His-X_3-Cys-X_2-Cys-X_6-Cys-X_2-Cys) were highly conserved in both monocots and dicots. However, the consensus sequence of *le* mutant was completely transformed by frameshift which was occurred by one nucleotide deletion. These results implicate that the functional roles of the LE orthologs are conserved in plants, and the complete destruction of C3HC4-type RING finger domain might loss the function protein.

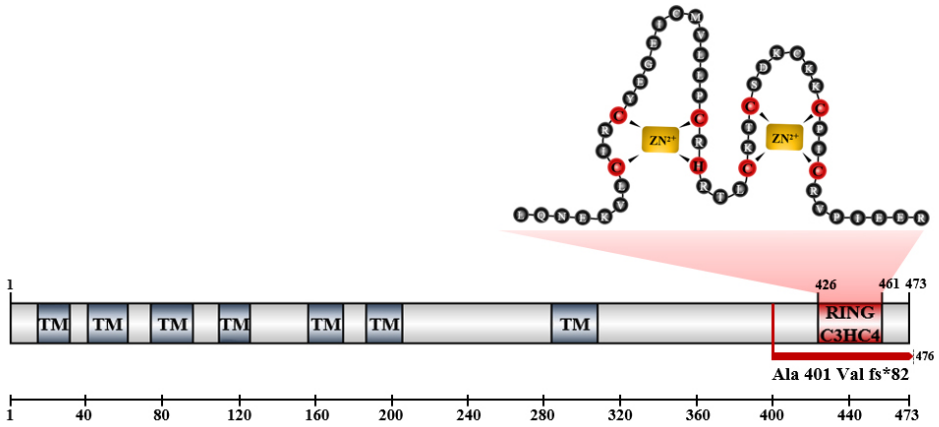

Figure 2-5. Schematic diagram of a C3HC4-type RING finger domain of LE. All amino acids indicate single-letter amino acid codes. Cysteines and histidine that bind the zinc ion are shown in red circle, and others are shown in black circle. TM, transmembrane domain.

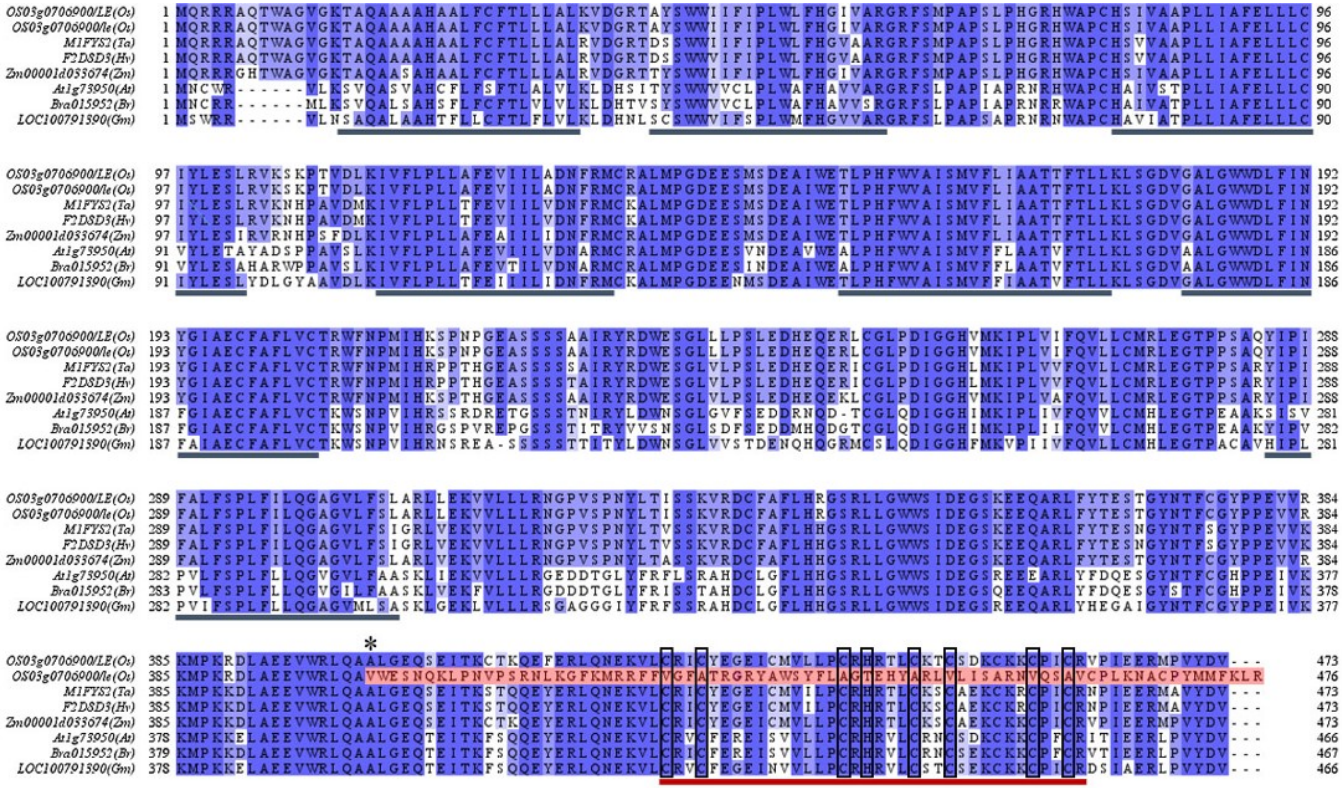

Figure 2-6. Multiple sequence alignment of LE orthologs. Asterisk represents the substituted residue caused by one base deletion in *le* mutant. Predicted transmembrane motifs, C3HC4-type RING domain, and conserved residues are highlighted in the alignment with blue and red lines, and black open boxes, respectively. Substituted amino acid residues by frameshift were highlighted by red background shading.

Expression Pattern of *LE*

To investigate expression pattern of *LE* gene, we performed qRT-PCR analysis and β-glucuronidase (GUS) staining in various organs of *LE* promoter::GUS transgenic plant (Fig. 2-7b). For qRT-PCR analysis, total RNA was extracted from various organ including leaf, stem, root, and seed in HC. Expression levels of *LE* were normalized to *UBIQUITIN5* and relative to expression in stem. *LE* was expressed in all investigated organs. The level of *LE* transcription is highest in the seed at 20 DAP and lowest in the stem. In seed development stage, *LE* showed relatively low expression at 5 DAP, but the expression increased at the late stage of seed development (Fig. 5a). The results of GUS staining were consistent with qRT-PCR results. GUS expression was observed in leaf, stem root, and seed (Fig. 5c-j). In early seed development stage, GUS was expressed in the inside part of pericarp (Fig. 5f-h), and the expression in pericarp was increased with seed growth.

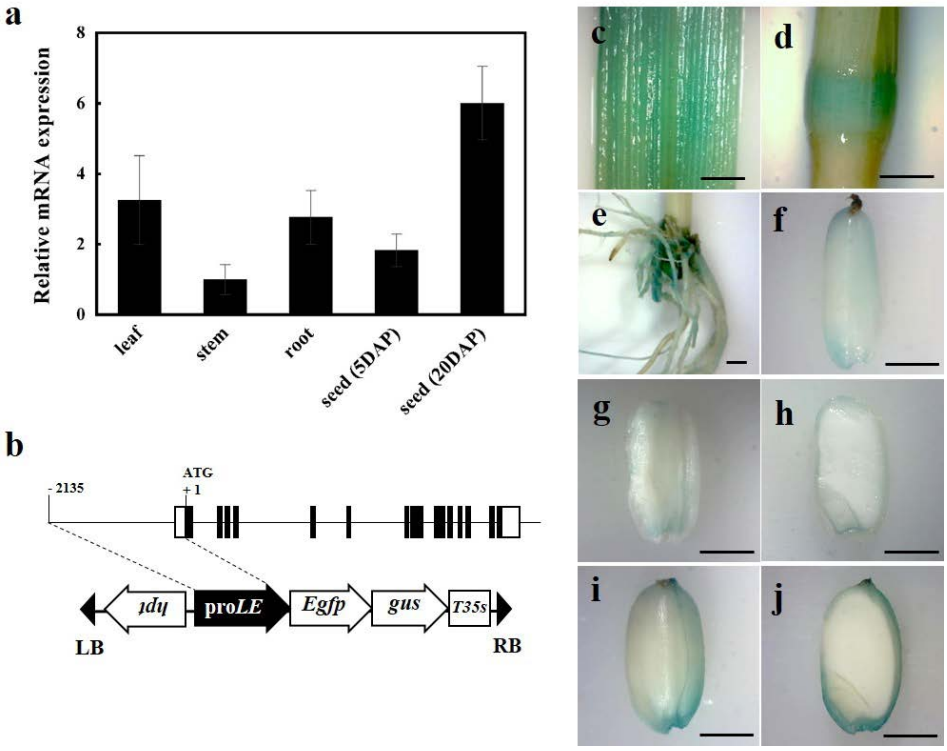

Figure 2-7. RNA expression pattern of *LE*. **a** Real-time PCR analysis of *LE* gene in leaf, stem, root and seed. **b** Construction of the *LE* promoter::GUS construct. **c-j** β-glucuronidase (GUS) expression pattern of various tissues in Pro*LE*::GUS transgenic line (**c**, leaf; **d**, stem; **e**, root; **f**, 5 DAP seed; **g** and **h**, 10 DAP seed; **i** and **j**, 20 DAP seed). Error bars indicate ± s.d. of replicates. Scale bar = 2 mm.

DISCUSSION

In characterization of three enlarged embryo mutants, the *ge* and *ge*^{s} mutant showed dramatic increase in EMW by 157% and 223% compared with wild type. Genetic analysis revealed that the responsible gene in *ge* and *ge*^{s} were allelic to *GE* located in chromosome 7. However, the *le* mutant of which EMW was increased by 48% more than wild type, was not allelic to the previously isolated genes, such as *GE* and *GO*.

LE encodes a C3HC4-type RING finger protein. LE protein consists of multi-transmembrane motifs and C3HC4-type RING domain. Cheung et al. (2007) had previously cloned and characterized *OsRHC1* which is identical to *LE*. *OsRHC1* was differentially expressed between bacterial blight resistant near-isogenic lines (NILs) containing the Xa14 or Xa23 and susceptible NILs by pathogen inoculation or wounding. In addition, overexpression of *OsRHC1* in transgenic Arabidopsis showed enhanced resistance to bacterial pathogens, which depended on the ubiquitin-mediated protein degradation. In rice, 29 C3HC4-type RING finger genes were identified by protein sequence analysis in silico (Takahashi et al. 2009). To date, the function of C3HC4-type RING finger genes in rice is much less understood. There are just a few reports that reveal the function of C3HC4-type RING finger gene such as OsCOP1, *OsCOIN1*, and *OsXB3* playing a role in photomorphogenesis,

tolerance of abiotic stress, and disease resistance, respectively (Tsuge et al. 2001; Liu et al. 2007; von Arnim and Deng 1993; Wang et al. 2006), but there is no report that C3HC4-type RING finger gene is involved in embryo morphology and development in rice. In Arabidopsis, the function of C3HC4-type RING finger genes is much more understood compared to rice, and many genes identified such as *AtCOP1* and *AtCIP8* (photomorphogenesis) (von Arnim and Deng 1993; Hardtke et al. 2002), *AtTED3* (light signaling) (Pepper and Chory 1997), *AtPEX10 and AtPEX12* (peroxisome biogenesis) (Schumann et al. 2003; Fan et al. 2005), *XBAT32* (root development), and *AtSDIR1* (stress tolerance) (Zhang et al. 2007). Interestingly, *AtPEX10* and *AtPEX12* consisting of two transmembrane helices and C3HC4-type RING finger domain, similar to *LE*, are required for peroxisome biogenesis and its dysfunction leads to lethality at the heart stage of embryogenesis.

Predicted LE is composed of seven transmembrane domain in the N-terminal and C3HC4-type RING domain in its C-terminal, and this composition shown to be essential for function and localization. Orthologs of *LE* were detected in both monocots and dicots and its amino acid sequences were highly conserved. In maize, developing seed cDNA library derived from developing seed was sequenced, which revealed that maize ortholog, *ZmZF13*, were expressed in developing seed (Wang et al. 2010a). However, there is apparently no published information on the functions of these orthologs, except pathogen defense of *OsRHC1*. Therefore, additional functional studies are needed to understand how *LE* gene works and regulates

embryo size.

As the embryo size was increased in order of *le*, *ge* and *ge*^{s}, GABA content of brown rice increased by 150%, 400%, and 850%, respectively. This results implicates that various nutrients and beneficial sources in embryo such as proteins, lipids, vitamins, minerals, and bioactive chemicals were also increased in enlarged embryo mutants. Therefore, Creation and discovery of new variation responsible for controlling embryo size is very important to manipulate embryo size based on the breeding purposes. If the target of breeding is related with bran or bran oil, the easier embryo detachment and the larger embryo size will be beneficial. On the other hand, if the purpose is improving nutritional quality with proper eating quality and milling, proper embryo size is needed. The *le* mutant is expected to be used as a breeding material to breed cultivars with a relatively high eating quality and unstriped embryo rate.

Generally, giant embryo mutant has shown problems in germination and seedling growth. The *go* mutant showed pleotropic phenotype with enlarge embryo, such as viviparous seed, shortened plastochron, and conversion of panicle primary branches to vegetative shoots (Kawakatsu et al. 2009). Similarly, the *ge* mutant also had defective seedling growth such as many malformed leaves and dwarfism which eventually cause death (Yang et al. 2013). The *le* mutant, on the other hand, had normal germination rate and seedling emergence. With these, the *le* mutant is expected to be used as promising breeding material for improving quality of rice and

cultivation problem such as low germination rate and seedling emergence, and lose of embryo during polishing process.

In this study, we identified *LE*, a new gene controlling embryo size, and its values as breeding material. The *le* mutant showed enlarged embryo phenotype which is relatively mild compared with *ge* mutant. *LE* encoded C3HC4-type RING finger protein, expecting new molecular mechanism to control embryo size. Although further studies are needed, our research provide novel insight and basis to understand molecular mechanism of embryo development and facilitate breeding new giant embryo rice cultivars.

REFERENCES

Aceto S, Gaudio L (2011) The MADS and the beauty: Genes involved in the development of orchid flowers, vol 12. doi:10.2174/138920211796429754

Acosta IF, Laparra H, Romero SP, Schmelz E, Hamberg M, Mottinger JP, Moreno MA, Dellaporta SL (2009) *tasselseed1* is a lipoxygenase affecting jasmonic acid signaling in sex determination of maize. Science (5911) 323:262-265

Ambrose BA, Lerner DR, Ciceri P, Padilla CM, Yanofsky MF, Schmidt RJ (2000) Molecular and genetic analyses of the *silky1* gene reveal conservation in floral organ specification between eudicots and monocots. Molecular Cell (3) 5:569-579

Buggenhout J, Brijs K, Celus I, Delcour JA (2013) The breakage susceptibility of raw and parboiled rice: A review. Journal of Food Engineering (3) 117:304-315

Cai Q, Yuan Z, Chen M, Yin C, Luo Z, Zhao X, Liang W, Hu J, Zhang D (2014) Jasmonic acid regulates spikelet development in rice. Nat Commun 5:3476

Caldelari D, Wang G, Farmer EE, Dong X (2011) Arabidopsis *lox3 lox4* double mutants are male sterile and defective in global proliferative arrest. Plant Molecular Biology (1) 75:25-33

Champagne ET, Wood DF, Juliano BO, Bechtel DB (2004) The rice grain and its gross composition. Rice chemistry and technology 3:77-107

Chen ZX, Wu JG, Ding WN, Chen HM, Wu P, Shi CH (2006) Morphogenesis and molecular basis on *naked seed rice*, a novel homeotic mutation of *OsMADS1* regulating transcript level of *AP3* homologue in rice. Planta (5) 223:882-890

Cheung MY, Zeng NY, Tong SW, Li FW, Zhao KJ, Zhang Q, Sun SS, Lam HM (2007) Expression of a RING-HC protein from rice improves resistance to *Pseudomonas syringae* pv. *tomato* DC3000 in transgenic *Arabidopsis thaliana*. J Exp Bot (15-16) 58:4147-4159

Chin JH, Kim JH, Jiang W, Chu SH, Woo MO, Han L, Brar D, Koh HJ (2007) Identification of subspecies-specific STS markers and their association with segregation distortion in rice (*Oryza sativa* L.). Journal of Crop Science and Biotechnology (3) 10:175-184

Choi I, Kim D, Son J, Yang C, Chun J, Kim K (2006) Physico-chemical Properties of Giant Embryo Brown Rice-Keunnunbyeo. Agricultural Chemistry and Biotechnology (3) 49:95

Chung S, Kim T, Rico C, Kang M (2014a) Effect of Instant Cooked Giant Embryonic Rice on Body Fat Weight and Plasma Lipid Profile in High Fat-Fed Mice. Nutrients (6) 6:2266

Chung SI, Lo LMP, Nam SJ, Jin X, Kang MY (2016a) Antioxidant Capacity of

Giant Embryo Rice Seonong 17 and Keunnunjami. JOAAT 3:94-98
Chung SI, Rico CW, Lee SC, Kang MY (2013) Hypolipidemic and Body Fat–Lowering Effects of Giant Embryo Brown Rice (Seonong 17 and Keunnunjami) in High-Fat-Fed Mice. Cereal Chemistry Journal (1) 91:18-22
Chung SI, Rico CW, Lee SC, Kang MY (2014b) Hypolipidemic and body fat–lowering effects of giant embryo brown rice (Seonong 17 and Keunnunjami) in high-fat-fed mice. Cereal Chemistry Journal (1) 91:18-22
Chung SI, Rico CW, Lee SC, Kang MY (2016b) Instant rice made from white and pigmented giant embryonic rice reduces lipid levels and body weight in high fat diet-fed mice. Obesity Research & Clinical Practice (6) 10:692-700
Debernardi JM, Lin H, Chuck G, Faris JD, Dubcovsky J (2017) microRNA172 plays a crucial role in wheat spike morphogenesis and grain threshability. Development (11) 144:1966-1975
Emanuelsson O, Nielsen H, von Heijne G (1999) ChloroP, a neural network-based method for predicting chloroplast transit peptides and their cleavage sites. Protein Sci (5) 8:978-984
Fan JL, Quan S, Orth T, Awai C, Chory J, Hu JP (2005) The arabidopsis *PEX12* gene is required for peroxisome biogenesis and is essential for development. Plant Physiology (1) 139:231-239
Faris JD, Fellers JP, Brooks SA, Gill BS (2003) A bacterial artificial chromosome contig spanning the major domestication locus *Q* in wheat and identification of a candidate gene. Genetics (1) 164:311-321
Faris JD, Gill BS (2002) Genomic targeting and high-resolution mapping of the domestication gene *Q* in wheat. Genome (4) 45:706-718
Fedak G, Tsuchiya T, Helgason SB (1972) Use of monotelotriomics for linkage mapping in barley. Canadian Journal of Genetics and Cytology (4) 14:949-957
Feussner I, Wasternack C (2002) The lipoxygenase pathway. Annual Review of Plant Biology (1) 53:275-297
Fitzgerald MA, McCouch SR, Hall RD (2009) Not just a grain of rice: the quest for quality. Trends in Plant Science (3) 14:133-139
Fu JR, Zhu LX, Sun XT, Zhou DH, Ouyang LJ, Bian JM, He HH, Xu J (2015) Genetic analysis of grain shape and weight after cutting rice husk. Genet Mol Res (4) 14:17739-17748
Garces R, Mancha M (1993) One-step lipid extraction and fatty acid methyl esters preparation from fresh plant tissues. Analytical Biochemistry (1) 211:139-143
Gopala Krishna A, Prabhakar J, Sen D (1984) Effect of degree of milling on tocopherol content of rice bran. Journal of Food Science and Technology (4) 21:222-224
Grechkin A (1998) Recent developments in biochemistry of the plant lipoxygenase pathway. Progress in Lipid Research (5) 37:317-352

Hakata M, Muramatsu M, Nakamura H, Hara N, Kishimoto M, Iida-Okada K, Kajikawa M, Imai-Toki N, Toki S, Nagamura Y, Yamakawa H, Ichikawa H (2017) Overexpression of TIFY genes promotes plant growth in rice through jasmonate signaling. Biosci Biotechnol Biochem (5) 81:906-913

Han SJ, Kwon SW, Chu S-H, Ryu SN (2012a) A New Rice Variety'Keunnunjami', with High Concentrations of Cyanidin 3-glucoside and Giant Embryo. Korean Journal of Breeding Science (2) 44

Han SJ, Kwon SW, Chu SH, Ryu SN (2012b) A new rice variety 'Keunnunjami', with high concentrations of cyanidin 3-glucoside and giant embryo. Korean Journal of Breeding Science (2) 44

Hardtke CS, Okamoto H, Stoop-Myer C, Deng XW (2002) Biochemical evidence for ubiquitin ligase activity of the *Arabidopsis* COP1 interacting protein 8 (CIP8). Plant J (4) 30:385-394

Hong H-C, Kim Y-G, Choi Y-H, Yang S-J, Lee K-S, Lee J-H, Jung O-Y, Yang C-I, Cho Y-C, Choi I-S (2012a) A Medium-Maturing, Giant-embryo, and Germination Brown Rice Cultivar'Keunnun'. Korean Journal of Breeding Science (2) 44

Hong HC, Kim YG, Choi YH, Yang SJ, Lee KS, Lee JH, Jung OY, Yang CI, Cho YC, Choi IS (2012b) A medium-maturing, giant-embryo, and germination brown rice cultivar'Keunnun'. Korean Journal of Breeding Science (2) 44

Hong SK, Aoki T, Kitano H, Satoh H, Nagato Y (1995a) Phenotypic diversity of 188 rice embryo mutants. Developmental Genetics (4) 16:298-310

Hong SK, Aoki T, Kitano H, Satoh H, Nagato Y (1995b) Temperature-sensitive mutation, embryoless-1, affects both embryo and endosperm development in rice. Plant Science (2) 108:165-172

Hong SK, Kitano H, Satoh H, Nagato Y (1996) How is embryo size genetically regulated in rice? Development (7) 122:2051-2058

Huang J, Cai M, Long Q, Liu L, Lin Q, Jiang L, Chen S, Wan J (2014) OsLOX2, a rice type I lipoxygenase, confers opposite effects on seed germination and longevity. Transgenic Research (4) 23:643-655

Huang R, Jiang L, Zheng J, Wang T, Wang H, Huang Y, Hong Z (2013) Genetic bases of rice grain shape: so many genes, so little known. Trends in Plant Science (4) 18:218-226

IRRI (1991) Rice genetics II: proceedings of the second international rice genetics symposium, 14-18 May 1990. International Rice Research Institute, Manila 1099, Philippines

Ishiguro S, Kawai-Oda A, Ueda J, Nishida I, Okada K (2001) The *DEFECTIVE IN ANTHER DEHISCENCE1* gene encodes a novel phospholipase A1 catalyzing the initial step of jasmonic acid biosynthesis, which synchronizes pollen maturation, anther dehiscence, and flower opening in arabidopsis. Plant Cell (10) 13:2191-2209

Jefferson RA, Kavanagh TA, Bevan MW (1987) GUS fusions: beta-glucuronidase

as a sensitive and versatile gene fusion marker in higher plants. The EMBO journal (13) 6:3901

Jeng TL, Shih YJ, Ho PT, Lai CC, Lin YW, Wang CS, Sung JM (2012) γ-Oryzanol, tocol and mineral compositions in different grain fractions of giant embryo rice mutants. Journal of the Science of Food and Agriculture (7) 92:1468-1474

Kawakatsu T, Taramino G, Itoh J, Allen J, Sato Y, Hong SK, Yule R, Nagasawa N, Kojima M, Kusaba M, Sakakibara H, Sakai H, Nagato Y (2009) *PLASTOCHRON3/GOLIATH* encodes a glutamate carboxypeptidase required for proper development in rice. Plant J (6) 58:1028-1040

Kim JY, Seo WD, Park DS, Jang KC, Choi KJ, Kim SY, Oh SH, Ra JE, Yi G, Park SK, Hwang UH, Song YC, Park BR, Park MJ, Kang HW, Nam MH, Han SI (2013) Comparative studies on major nutritional components of black waxy rice with giant embryos and its rice bran. Food Science and Biotechnology (1) 22:121-128

Kim KH, Heu MH, Park SZ, Koh HJ (1991) New mutants for endosperm and embryo characters in rice. Korean Journal of Crop Science (3) 36:197-203

Koh H, Won Y, Heu M, Park S (1993a) Nutritional and agronomic characteristics of super-giant embryo mutant in rice. Korean Journal of Crop Science 38

Koh HJ, Heu MH (1994) Physicochemical properties of sugary-endosperm mutants in rice. Korean Journal of Crop Science (1) 39:1-6

Koh HJ, Heu MH, McCouch SR (1996) Molecular mapping of the *ge (s)* gene controlling the super-giant embryo character in rice (*Oryza sativa* L.). Theor Appl Genet (1-2) 93:257-261

Koh HJ, Park SZ, Won YJ, Heu MH (1993b) Nutritional and agronomic characteristics of super-giant embryo mutant in rice. Korean Journal of Crop Science (6) 38:537-544

Kolthoff IM, Sandell EB (1952) Textbook of quantitative inorganic analysis. 3rd edn. Macmillan & Co., New York

Krizek BA, Fletcher JC (2005) Molecular mechanisms of flower development: an armchair guide. Nat Rev Genet (9) 6:688-698

Kumar S, Sangwan P, Dhankhar RMV, Bidra S (2013) Utilization of rice husk and their ash: A review. Res J Chem Env Sci (5) 1:126-129

Lee CP, Chin JH, Cho YI, Koh HJ (2004) Grain characteristics and inheritance of two split-hull mutants in rice. Korean Journal of Breeding (3) 16:146-150

Lee G (2013) Genetic mapping of giant embryo mutant and varietal variation of rice embryo. Masters dissertation, Seoul National University, Korea

Lee KI (2012) Phenotypic characterization and genetic mapping of split-hull mutant in rice. Masters dissertation, Seoul National University, Korea

Liavonchanka A, Feussner I (2006) Lipoxygenases: Occurrence, functions and catalysis. Journal of Plant Physiology (3) 163:348-357

Liu K, Wang L, Xu Y, Chen N, Ma Q, Li F, Chong K (2007) Overexpression of

OsCOIN, a putative cold inducible zinc finger protein, increased tolerance to chilling, salt and drought, and enhanced proline level in rice. Planta (4) 226:1007-1016

Liu LL, Zhai HQ, Wan JM (2005) Accumulation of gamma-aminobutyric acid in giant-embryo rice grain in relation to glutamate decarboxylase activity and its gene expression during water soaking. Cereal Chemistry (2) 82:191-196

Lombardo F, Yoshida H (2015) Interpreting lemma and palea homologies: a point of view from rice floral mutants. Frontiers in Plant Science (61) 6

Maeda H, Nemoto H, Iida S, Ishii T, Nakagawa N, Hoshino T, Sakai M, Okamoto M, Shinoda H, Yoshida T (2001) A new rice variety with giant embryos, "Haiminori". Breeding Science (3) 51:211-213

Michelmore RW, Paran I, Kesseli RV (1991) Identification of markers linked to disease-resistance genes by bulked segregant analysis - a rapid method to detect markers in specific genomic regions by using segregating populations. Proceedings of the National Academy of Sciences of the United States of America (21) 88:9828-9832

Miko I (2008) Phenotype variability: penetrance and expressivity. Nature Education (1) 1:137

Nagasawa N (2003) *SUPERWOMAN1* and *DROOPING LEAF* genes control floral organ identity in rice. Development (4) 130:705-718

Nagasawa N, Hibara K, Heppard EP, Vander Velden KA, Luck S, Beatty M, Nagato Y, Sakai H (2013) *GIANT EMBRYO* encodes CYP78A13, required for proper size balance between embryo and endosperm in rice. Plant J (4) 75:592-605

Nishimura A, Aichi I, Matsuoka M (2007) A protocol for agrobacterium-mediated transformation in rice. Nat Protocols (6) 1:2796-2802

Ohmori S, Kimizu M, Sugita M, Miyao A, Hirochika H, Uchida E, Nagato Y, Yoshida H (2009) *MOSAIC FLORAL ORGANS1*, an AGL6-like MADS box gene, regulates floral organ identity and meristem fate in rice. The Plant Cell (10) 21:3008-3025

Ohta H, Shida K, Peng Y-L, Furusawa I, Shishiyama J, Aibara S, Morita Y (1991) A lipoxygenase pathway is activated in rice after infection with the rice blast fungus *Magnaporthe grisea*. Plant Physiology (1) 97:94-98

Ougham HJ, Latipova G, Valentine J (1996) Morphological and biochemical characterization of spikelet development in naked oats (*Avena sativa*). New Phytologist (1) 134:5-12

Park JH, Halitschke R, Kim HB, Baldwin IT, Feldmann KA, Feyereisen R (2002) A knock-out mutation in allene oxide synthase results in male sterility and defective wound signal transduction in *Arabidopsis* due to a block in jasmonic acid biosynthesis. The Plant Journal (1) 31:1-12

Pauwels L, Morreel K, De Witte E, Lammertyn F, Van Montagu M, Boerjan W, Inzé D, Goossens A (2008) Mapping methyl jasmonate-mediated

transcriptional reprogramming of metabolism and cell cycle progression in cultured *Arabidopsis* cells. Proceedings of the National Academy of Sciences (4) 105:1380-1385

Pedersen JF, Vogel KP, Funnell DL (2005) Impact of reduced lignin on plant fitness. Crop Science (3) 45:812

Pepper AE, Chory J (1997) Extragenic suppressors of the arabidopsis *det1* mutant identify elements of flowering-time and light-response regulatory pathways. Genetics (4) 145:1125-1137

Sakata M, Seno M, Matsusaka H, Takahashi K, Nakamura Y, Yamagata Y, Angeles ER, Mochizuki T, Kumamaru T, Sato M, Enomoto A, Tashiro K, Kuhara S, Satoh H, Yoshimura A (2016) Development and evaluation of rice giant embryo mutants for high oil content originated from a high-yielding cultivar 'Mizuhochikara'. Breed Sci (3) 66:425-433

Salzman RA, Brady JA, Finlayson SA, Buchanan CD, Summer EJ, Sun F, Klein PE, Klein RR, Pratt LH, Cordonnier-Pratt M-M, Mullet JE (2005a) Transcriptional Profiling of Sorghum Induced by Methyl Jasmonate, Salicylic Acid, and Aminocyclopropane Carboxylic Acid Reveals Cooperative Regulation and Novel Gene Responses. Plant Physiol (1) 138:352-368

Salzman RA, Brady JA, Finlayson SA, Buchanan CD, Summer EJ, Sun F, Klein PE, Klein RR, Pratt LH, Cordonnier-Pratt MM, Mullet JE (2005b) Transcriptional profiling of sorghum induced by methyl jasmonate, salicylic acid, and aminocyclopropane carboxylic acid reveals cooperative regulation and novel gene responses. Plant Physiol (1) 138:352-368

Satoh H, Iwata N (1990) Linkage analysis in rice. On three mutant loci for endosperm properties, *ge* (*giant embryo*), *du-4* (*dull endosperm-4*) and *flo-1* (*floury endosperm-1*). Japan J Breed (Suppl 2) 40:268-269

Satoh H, Omura T (1981a) New Endosperm Mutations Induced by Chemical Mutagens in Rice, Oryza-Sativa-L. Japanese Journal of Breeding (3) 31:316-326

Satoh H, Omura T (1981b) New endosperm mutations induced by chemical mutagens in rice, *Oryza Sativa* L. Japanese Journal of Breeding (3) 31:316-326

Schumann U, Wanner G, Veenhuis M, Schmid M, Gietl C (2003) AthPEX10, a nuclear gene essential for peroxisome and storage organelle formation during *Arabidopsis* embryogenesis. Proc Natl Acad Sci U S A (16) 100:9626-9631

Schwarz-Sommer Z, Huijser P, Nacken W, Saedler H, Sommer H (1990) Genetic control of flower development by homeotic genes in *Antirrhinum majus*. Science (4983) 250:931-936

Si L, Chen J, Huang X, Gong H, Luo J, Hou Q, Zhou T, Lu T, Zhu J, Shangguan Y, Chen E, Gong C, Zhao Q, Jing Y, Zhao Y, Li Y, Cui L, Fan D, Lu Y, Weng

Q, Wang Y, Zhan Q, Liu K, Wei X, An K, An G, Han B (2016) *OsSPL13* controls grain size in cultivated rice. Nat Genet (4) 48:447-456
Siedow JN (1991) Plant lipoxygenase: structure and function. Annual Review of Plant Physiology and Plant Molecular Biology (1) 42:145-188
Simons KJ, Fellers JP, Trick HN, Zhang Z, Tai YS, Gill BS, Faris JD (2006) Molecular characterization of the major wheat domestication gene *Q*. Genetics (1) 172:547-555
Smith CW, Dilday RH (2003) Rice : origin, history, technology, and production. Hoboken, NJ : John Wiley & Sons, Hoboken, NJ
Sormacheva I, Golovnina K, Vavilova V, Kosuge K, Watanabe N, Blinov A, Goncharov NP (2014) *Q* gene variability in wheat species with different spike morphology. Genetic Resources and Crop Evolution (6) 62:837-852
Stintzi A, Browse J (2000) The *Arabidopsis* male-sterile mutant, *opr3*, lacks the 12-oxophytodienoic acid reductase required for jasmonate synthesis. Proceedings of the National Academy of Sciences of the United States of America (19) 97:10625-10630
Suzuki Y, Ise K, Li C, Honda I, Iwai Y, Matsukura U (1999a) Volatile components in stored rice (*Oryza sativa* L.) of varieties with and without lipoxygenase-3 in seeds. Journal of Agricultural and Food Chemistry (3) 47:1119-1124
Suzuki Y, Ise K, Li C, Honda I, Iwai Y, Matsukura U (1999b) Volatile components in stored rice [*Oryza sativa* (L.)] of varieties with and without lipoxygenase-3 in seeds. Journal of Agricultural and Food Chemistry (3) 47:1119-1124
Swamy YMI, Bhattacharya KR (1979) Breakage of rice during milling effect of kernel deffects and grain demension. Journal of Food Process Engineering (1) 3:29-42
Takahashi S, Ohtani T, Iida S, Sunohara Y, Matsushita K, Maeda H, Tanetani Y, Kawai K, Kawamukai M, Kadowaki K-i (2009) Development of CoQ10-enriched rice from giant embryo lines. Breeding science (3) 59:321-326
Takeda K, Takahashi M-E (1970) Unbalanced growth in floral glumes and caryopsis in rice. : I. Varietal difference in the degree of unbalance and the occurrence of mulformed grains. (Genetical Studies on Rice Plant, XXXXV). Japanese Journal of Breeding (6) 20:337-343
Taketa S, Amano S, Tsujino Y, Sato T, Saisho D, Kakeda K, Nomura M, Suzuki T, Matsumoto T, Sato K, Kanamori H, Kawasaki S, Takeda K (2008) Barley grain with adhering hulls is controlled by an ERF family transcription factor gene regulating a lipid biosynthesis pathway. Proceedings of the National Academy of Sciences (10) 105:4062-4067
Tanaka K, Ogawa M, Kasai Z (1977) rice scutellum. II. A comparison of scutellar and aleurone electron dense particles by transmission electron microscopy including energy dispersive X ray analysis. Cereal chemistry
Taramino G, Allen J, Hong S, Nagasawa N, Nagato Y, Sakai H (2003) Mapping of *GOLIATH*, a new gene controlling embryo size in rice. Rice Genet Newsl

20:24-27
Tsuge T, Inagaki N, Yoshizumi T, Shimada H, Kawamoto T, Matsuki R, Yamamoto N, Matsui M (2001) Phytochrome-mediated control of *COP1* gene expression in rice plants. Mol Genet Genomics (1) 265:43-50
Ubert IP, Zimmer CM, Pellizzaro K, Federizzi LC, Nava IC (2017) Genetics and molecular mapping of the naked grains in hexaploid oat. Euphytica (2) 213
von Arnim AG, Deng XW (1993) Ring finger motif of *Arabidopsis thaliana* COP1 defines a new class of zinc-binding domain. J Biol Chem (26) 268:19626-19631
von Malek B, van der Graaff E, Schneitz K, Keller B (2002) The *Arabidopsis* male-sterile mutant *dde2-2* is defective in the *ALLENE OXIDE SYNTHASE* gene encoding one of the key enzymes of the jasmonic acid biosynthesis pathway. Planta (1) 216:187-192
Wang G, Wang H, Zhu J, Zhang J, Zhang X, Wang F, Tang Y, Mei B, Xu Z, Song R (2010a) An expression analysis of 57 transcription factors derived from ESTs of developing seeds in Maize (*Zea mays*). Plant Cell Rep (6) 29:545-559
Wang K, Tang D, Hong L, Xu W, Huang J, Li M, Gu M, Xue Y, Cheng Z (2010b) *DEP* and *AFO* regulate reproductive habit in rice. PLoS Genetics (1) 6:e1000818
Wang S, Li S, Liu Q, Wu K, Zhang J, Wang S, Wang Y, Chen X, Zhang Y, Gao C, Wang F, Huang H, Fu X (2015) The *OsSPL16-GW7* regulatory module determines grain shape and simultaneously improves rice yield and grain quality. Nat Genet (8) 47:949-954
Wang YS, Pi LY, Chen X, Chakrabarty PK, Jiang J, De Leon AL, Liu GZ, Li L, Benny U, Oard J, Ronald PC, Song WY (2006) Rice XA21 binding protein 3 is a ubiquitin ligase required for full *Xa21*-mediated disease resistance. Plant Cell (12) 18:3635-3646
Wasternack C, Hause B (2013) Jasmonates: biosynthesis, perception, signal transduction and action in plant stress response, growth and development. An update to the 2007 review in Annals of Botany. Annals of Botany (6) 111:1021-1058
Yan Y, Borrego E, Kolomiets MV (2013) Jasmonate biosynthesis, perception and function in plant development and stress responses. In: Baez RV (ed) Lipid Metabolism. InTech, Rijeka, p Ch. 16. doi:10.5772/52675
Yang DW, Ye XF, Zheng XH, Cheng CP, Ye N, Lu LB, Huang FH, Li QQ (2016) Identification and fine mapping of *lemma-distortion1*, a single recessive gene playing an essential role in the development of lemma in rice. J Agric Sci (06) 154:989-1001
Yang W, Gao M, Yin X, Liu J, Xu Y, Zeng L, Li Q, Zhang S, Wang J, Zhang X, He Z (2013) Control of rice embryo development, shoot apical meristem maintenance, and grain yield by a novel cytochrome p450. Mol Plant (6)

6:1945-1960
Yoshida H, Nagato Y (2011) Flower development in rice. Journal of Experimental Botany (14) 62:4719-4730
Yu J, Xiong H, Zhu X, Zhang H, Li H, Miao J, Wang W, Tang Z, Zhang Z, Yao G, Zhang Q, Pan Y, Wang X, Rashid MAR, Li J, Gao Y, Li Z, Yang W, Fu X, Li Z (2017) *OsLG3* contributing to rice grain length and yield was mined by Ho-LAMap. BMC Biol (1) 15:28
Yuan Z, Gao S, Xue DW, Luo D, Li LT, Ding SY, Yao X, Wilson ZA, Qian Q, Zhang DB (2009) *RETARDED PALEA1* controls palea development and floral zygomorphy in rice. Plant Physiology (1) 149:235-244
Zhang L, Hu P, Tang S, Zhao H, Wu D (2005) Comparative studies on major nutritional components of rice with a giant embryo and a normal embryo. Journal of Food Biochemistry (6) 29:653-661
Zhang P, Allen WB, Nagasawa N, Ching AS, Heppard EP, Li H, Hao X, Li X, Yang X, Yan J, Nagato Y, Sakai H, Shen B, Li J (2012) A transposable element insertion within *ZmGE2* gene is associated with increase in embryo to endosperm ratio in maize. Theor Appl Genet (7) 125:1463-1471
Zhang Y, Yang C, Li Y, Zheng N, Chen H, Zhao Q, Gao T, Guo H, Xie Q (2007) *SDIR1* is a RING finger E3 ligase that positively regulates stress-responsive abscisic acid signaling in *Arabidopsis*. Plant Cell (6) 19:1912-1929
Zhao GC, Xie MX, Wang YC, Li JY (2017) Molecular Mechanisms Underlying gamma-Aminobutyric Acid (GABA) Accumulation in Giant Embryo Rice Seeds. J Agric Food Chem (24) 65:4883-4889
Zhou G, Ren N, Qi J, Lu J, Xiang C, Ju H, Cheng J, Lou Y (2014) The 9-lipoxygenase Osr9-LOX1 interacts with the 13-lipoxygenase-mediated pathway to regulate resistance to chewing and piercing-sucking herbivores in rice. Physiologia Plantarum (1) 152:59-69

초 록

벼의 개영(*SPLIT-HULL*) 유전자와 중거대배(*LARGE EMBRYO*) 유전자의 동정

벼는 90% 이상의 아시아인들, 그리고 세계인구의 50% 이상이 주식으로 사용하는 주요 식량작물 중 하나이다. 벼에서 식량으로 이용되는 부분은 종자이기 때문에 화기의 형성에서부터 종자 등숙에 이르기까지의 모든 종자의 발달과정은 벼 육종 및 유전 연구에 있어서 매우 중요한 주제 중 하나이다. 본 연구에서는 종자 발달에 관련된 유전자를 동정하고 육종적 이용가능성을 확인하고자 벼 개영(*split-hull*) 돌연변이체와 중거대배(*large embryo*) 돌연변이체에 대한 형태적 특성 조사 및 염색체 지도 기반 유전자 동정실험을 진행하였다.

벼 종자는 종자 외부를 감싸고 있는 영과 알맹이로 이루어져 있다. 포엽과 유사한 형태의 두 개의 기관인 외영과 내영으로 이루어져 있는 영은 종자 발달 과정 동안 외부 환경으로부터 내부의 화기와 발달 중인 종자를 보호하고 종자의 모양과 크기를 결정하는 중요한 역할을 한다. 벼 개영 돌연변이체는 종자가

등숙함에 따라 외영과 내영의 연결부위가 터지는 표현형을 나타낸다. 개영 돌연변이체의 형태 및 물리적 특성 조사를 통해 정상개체와 비교하였을 때 외영의 폭이 감소하였으며 영의 세포 내 리그닌 함량이 감소하였다. 이를 통해 리그닌 감소에 따른 영의 강도 약화와 외영의 폭 감소가 영이 터지는 표현형을 야기할 것이라 추정하였다. 개영 유전자(*SPH*)는 4번염색체에 위치하고 있었으며 type-2의 13-lipoxygenase를 암호화하고 있었다. *SPH* 유전자는 잎, 뿌리, 줄기, 영화에서 모두 발현하였으며 특히 영이 갈라짐이 발생하는 외영의 말단 고리 부위에서도 발현이 관찰되었다. *SPH* 발현 억제 및 정지 형질전환체들의 표현형을 조사한 결과, 개영 돌연변이체와 동일하게 영이 터지는 표현형을 나타냈으며, 영화의 리놀산과 리놀렌산의 함량이 정상벼에 비해 개영 돌연변이체에서 높게 측정되었다. 이를 통해 영이 터지는 표현형이 *SPH* 유전자의 결함에 의해 발생한다는 것을 확인하였다. 육종적 이용가능성을 알아보기 위해 실시한 제현실험 결과, 개영 돌연변이체는 정상벼에 비해 낮은 제현강도에서도 높은 제현율을 나타냈으며, 이런 특성은 제현 시 싸라기가 쉽게 발생하는 벼 품종을 개선하는데 이용될 수 있을 것으로 기대된다.

배는 벼 종자에서 가장 적은 부분을 차지하지만 매우 높은 영양적 가치를 가진다. 배 크기 조절은 벼의 영양학적 질을 획기적으로 개선시킬 수 있는 육종 전략 중에 하나이다. 2장의 연구에서는 배의 크기 증가 정도에 따라 *le*, *ge*, *ge*^{s}로 명명된 세 개의 거대 배 돌연변이를 이용해 특성조사 및 유전분석을 진행하였다. 거대배 돌연변이체들은 배 크기의 증가와 함께 GABA 함량이 증가하는 정의 상관관계를 보였다. 정역교배를 통한 대립성검정과 기존에 보고된 거대배 유전자좌의 염기서열분석을 통해 *ge*와 *ge*^{s}는 기존에 보고된 거대배 유전자인 *GE*의 대립유전자인 것으로 확인되었고, 이와 달리 중거대배(*le*) 돌연변이체의 배 크기 증가는 새로운 하나의 유전자에 의해 조절된다는 것을 확인하였다. *LE* 유전자를 찾기 위해 유전자 지도에 기초한 유전자 분리를 진행한 결과, 3번 염색체에 위치한 *OS03g0706900*에서 틀 이동 돌연변이를 유발하는 하나의 염기서열 결손을 발견하였다. 이 유전자는 C3HC4-type RING finger 도메인을 갖는 단백질을 암호화하고 있었으며 *LE* 발현 억제 형질전체를 만들어 확인한 결과 배의 크기가 증가한 돌연변이체 표현형을 나타냈다. 이를 통해 C3HC4-type RING finger 단백질이 벼의 배 크기 조절에 관여한다는 것을 확인 할 수

있었다. *LE* 유전자는 잎, 줄기, 뿌리, 종자에서 모두 발현하는 것으로 나타났으며 특히 수분 후 20일된 종자에서 가장 높은 발현을 나타냈다. 이러한 연구결과들은 벼의 배 크기를 조절하는 새로운 기작에 대한 기초 정보를 제공하며 추가적인 연구를 통해 배 크기 조절 기작에 대한 이해를 높이고 *le* 돌연변이체를 이용한 새로운 거대배 벼 품종육성도 가능할 것으로 기대된다.